



BIOMACH



Project no. **[505487-1]**

Project acronym: **BIOMACH**

Project full name: **“Molecular Machines – Design and Nano-Scale Handling of Biological Antetypes and Artificial Mimics“**

Instrument type: **SPECIFIC TARGETED RESEARCH PROJECT**

Priority name: [NMP-2002-3.4.1.1-3: Molecular and bio-molecular mechanisms and engines]

## **MID-TERM REVIEW REPORT**

Period covered: from **01.03.2004** to **31.08.2005** Date of submission: **05.09.2005**

Start date of project: **01.03.2004**

Duration: **3 years**

Project coordinator name:

Project coordinator organisation name:

**Dr. Mario Ruben  
Institute of Nanotechnology  
Research Centre Karlsruhe**

## Summary

The BIOMACH–Project has achieved within the first 18-months funding period (from March 2003 to September 2005) the following results:

- establishing of a guiding management framework (BIOMACH project office, BIOMACH website)
- initiation of the scientific discussion (23 meetings at different levels of participation)
- start of several scientific cross-disciplinary collaborations
- delivering in time of five deliverables, twelve milestones, two reports and seven financial audits
- organisation of the Mid-term review meeting conference as an international workshop from 18<sup>th</sup> to 23<sup>rd</sup> September 2005 in Ascona/Switzerland

Based on the so far obtained results, it can be stated that cutting-edge research as leading European contribution to the fast developing field of “Molecular Motors” has been achieved during the first funding period. For the upcoming second funding period, an even increased output of scientific production is expected to be delivered by the BIOMACH consortium.

## Table of Contents

<b>Summary</b>	<b>1</b>
<b>Scientific Progress and Collaborative Achievements of BIOMACH</b>	<b>3</b>
<b>Workpackage 1 - NANOHANDLING</b>	<b>7</b>
<b>Workpackage 2 - SELF-ASSEMBLY</b>	<b>11</b>
<b>Workpackage 3 - ELECTROENGINES</b>	<b>15</b>
<b>Workpackage 4 – PHOTOCHEMICAL DEVICES</b>	<b>20</b>
<b>Workpackage 5 – NANOPORE MACHINES</b>	<b>26</b>
<b>Workpackage 6 – BIOMOLECULAR MOTORS</b>	<b>34</b>
<b>Conclusion</b>	<b>39</b>
<b>Plan for the dissemination of knowledge</b>	<b>40</b>

### **Annex I: Deliverables list**

**Deliverable D4-2**

**Deliverable D5-1**

### **Annex II: Publication list**

## Scientific Progress and Collaborative Achievements of BIOMACH

The first 18 months-period of the cross-disciplinary research initiative BIOMACH has been mainly marked by approaching of before mainly separately acting different scientific communities (Physics, Chemistry, Theory and Biology), although all dealing with molecular machines. This step-wise process was initiated by a multitude of scientific meetings (in total 23) at different levels of participation and resulted finally in the set-up of several cross-disciplinary two- or three-centre collaborations. Since any collaborative contact between the partners of the BIOMACH consortium did not exist before the creation of the BIOMACH project, the importance and the sensitivity of the formation process for the success of the project should be underlined here. In general, the partners of the six work packages (WP 1: Nanohandling, WP 2: Self-Assembly, WP 3: Electroengines, WP 4: Photochemical Devices, WP 5 Nanopore Machines, WP 6: Biomolecular Motors), worked mainly along the scientifically given objectives (see Annex I) and fulfilled or partially fulfilled 12 milestones and five deliverables. The details of the **scientific progress** within the work packages are reported below.

### BIOMACH Workpackages Progress - Plan and Status M01-M18 (MTRM)

		<i>start months</i>							<i>MTRM</i>
<b>WORKPACKAGES</b>	tool	0	3	6.	9	12	15	18	
WP1 Nano-Handling	<b>D</b>								
	<b>M</b>				<b>M1-1</b>			<b>M1-2</b>	
WP2 Self-Assembly	<b>D</b>								
	<b>M</b>					<b>M2-1/2</b>			
WP3 Electro Engines	<b>D</b>					<b>D3-1</b>			
	<b>M</b>			<b>M3-1</b>		<b>M3-2</b>			
WP4 Photochemical Engines	<b>D</b>					<b>D4-1</b>		<b>D4-2</b>	
	<b>M</b>			<b>M4-1</b>		<b>M4-2</b>		<b>M4-3</b>	
WP5 Nanopore Machines	<b>D</b>							<b>D5-1</b>	
	<b>M</b>			<b>M5-1</b>		<b>M5-2</b>		<b>M5-3</b>	
WP6 Biomolecular Motors	<b>D</b>					<b>D6-1</b>			
	<b>M</b>			<b>M6-1</b>		<b>M6-2</b>			

**D**- Deliverable; **M**- Milestone,

**MTRM**- Mid-term Review Meeting

**DMa1: Intern. conference**

**DMa2: BIOMACH website**

From the **management** point of view, the BIOMACH consortium can report on the fulfillment of the two Management deliverables (**DMa 1** “BIOMACH conference of on nanomotors and bioengines (M18)”; in conclusion to the Mid-Term Review meeting, and **DMa 2** “Creation of the BIOMACH website (M18)”, preliminarily delivered in M09). In addition, the M12 Periodic Activity and Management reports in combination with the respective audit certificates were delivered in time, although some revisions and clearings had been necessary. The **dissemination of the created knowledge** to a broader public was guaranteed by the anticipated set-up of the BIOMACH website (M09 instead M18) and by the publication of three different press releases.

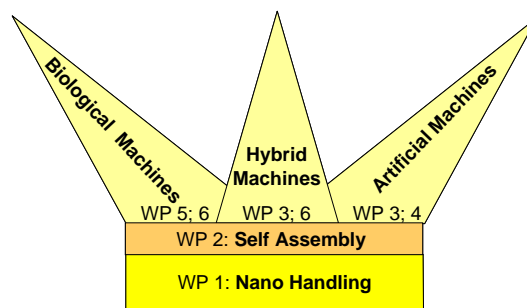


Figure 1: Scheme of the scientific structure of the BIOMACH project

Due to its fundamental role within the project, the **WP 1 - Nanohandling** (see Figure 1) has been experienced the strongest collaborative effort, so far. In order to realize **M 1-1** “Identification of functionalized rotaxane and ring units grafted at surfaces (M08)”, a two-centre **collaboration** consisting of the partners **MPI-FKF** and **ULP** has achieved the fixation of motor units at silver surfaces and their single-molecule STM-observation. Additionally and in fulfilling **M 1-2** “Control of LFMC’s oriented at surfaces (M16)”, simple photoactive organic compounds could be self-assembled onto surfaces by different techniques (sublimation and surfaces-assisted coordination, see also WP 4). Parallely and in accordance with the general objectives of WP 1, the groups **MPI-FKF** and **AMOLF** have been pursued the development of new techniques for the handling, positioning, observation and operation of molecular machines and their units at the single-molecule level. Especially, the combination of STM techniques with technological set-ups introducing electromagnetical fields is of highest importance laying a necessary instrumental base for the planned experiments in WP 3, 4 and 5 concerning alternative fueling techniques as photons or electrons.

The **WP 2 – Self-Assembly** has dealt with the in-situ build-up of artificial motors from separated components and consists basically of two independent research lines. One line is working under UHV condition on surfaces and is dealing with the **M2-1** “Synthesis of the scaffold for the Au-Anchoring (M12)” and with the **M2-2** “Synthesis of the modified rotary motor units and their self-assembly (M12)”. Both milestones could be reached, in strong overlap with WP 1 and 3, by the realisation of a supramolecular scaffold and the subsequent positioning of the respective motor units into the open voids thus avoiding the before observed formation of tetramers and dimers of the motor units (see WP 1). This research results could be only obtained by the joint scientific effort of the BIOMACH-partners **FZK-INT** (scaffold), **ULP** (motor units) and **MPI-FKF** (STM-imaging). Additional work of the **EPFL** partner explored further self-assembly approaches of simple organic molecules at metallic surfaces. The second research line within WP 2 is on the way to investigate the synthesis of chiral and semi-conducting scaffolds (M2-3 and 2-4 due to M20 and M24) in solution. This work is mainly driven by the BIOMACH-partner **Tu/e** and it is planned to merge the two complementary research lines against the end of the BIOMACH-project.

The **WP 3 – Electroengines** is mainly investigating the possibility to modify and to adapt already known rotaxane units and motors (which are have been proven to be fully operable in solution) to surface conditions. Towards this goal, the respective molecules had to be modified and to be resynthesized (**M3-1** “Synthesis of a switchable rotaxane unit bearing the appropriated functional group for grafting (M06)) and studying its grafting behaviour on surfaces (**M3-2** (M12)). These research efforts were described in detail in the deliverable **D3-1** “Controlled grafting of catenane and rotaxane units at metal surfaces (M12)” based on work mainly achieved by BIOMACH-partner **ULP**. However, the recent research effort carried out on silver surfaces by the **research collaboration FZK-INT/ ULP/ MPI-FKF** in WP 1 and 2 point eventually to an alternative way towards surface-grafted molecular rotators (vide infra).

Additionally, the build-up of an STM set-up working under solution condition and where an external electric field can be included (see WP1) constitute a necessary technical prerequisite to test the possibility of electrochemically induced rotation motion with artificial rotator systems.

The objective of the **WP 4 – Photochemical Devices** is to integrate light-fueled molecular components (LFMC's) into artificial nanomotors as an alternative fueling strategy. This objective was approached by investigating two types of systems. First, the shuttling of a molecular ring along a dumbbell component in a rotaxane caused by a photoinduced sequence of electron-transfer processes was investigated. Within the work towards **M4-1** "Synthesis of a LFMC (M12)" and **M4-2** "Photophysical characterization of LFMC's in solution (M12)", detailed spectroscopic investigations allowed BIOMACH-partner **CIAM** to show that the investigated rotaxane behaves as an autonomous nanomotor driven by visible light in solution, albeit with a rather low efficiency. Computational simulations of the system carried out by BIOMACH-partner **ETH** have started to unravel the mechanism of the shuttling process, and are expected to be crucial for the design of novel prototypes with improved performance. This work was described in detail within the deliverables **D4-1** "Final Design of a light-fueled molecular component (M12)" and **D4-2** "Computational treatment of light-induced rotary movements in LFMC's (M18)" and will be proceeded in close cooperation between **CIAM** and **ETH**. Secondly, the *trans-cis* photoisomerization of an azobenzene derivative as LFMC on a metal surface was investigated in order to reach milestone **M4-3** "Self-assembly of LFMC's on surfaces (M16)". The experiments, performed by **FZK-INT** in collaboration with **MPI-FKF**, showed that the azobenzene LFMC's can be deposited as a monolayer onto a Cu(100) surface by sublimation under UHV conditions. The subnanometer-scale STM topographic studies of the surface revealed that domains of the *trans*-isomer are formed. Photoisomerization studies on such molecules under near-surface conditions are underway.

In **WP 5 -Nanopore Machines**, the determination of the translocation activity on surfaces, specific and strong linkages of the protein and vesicles to beads has been achieved, fulfilling the milestones (**M5-1** "Establish efficient translocation into vesicles on a surface (M06)" and **M5-2** "Establish a procedure to firm attachment of vesicles to surfaces(M14)") and the obtained results were concluded in **D5-1** "Modification of the vesicles and proteins involved in protein-importing molecular motors (M18)" by the BIOMACH partner **AMOLF**. This results represent the platform to attack the central objective of WP5, the fully comprehension of the bacterial Sec system, which is considered as a model system for many others protein importing systems. After realizing further improvements to the aspecific P8-vesicle interactions, BIOMACH can start looking for movements generated by the protein translocation machinery. Towards this goal, computational studies were carried out by BIOMACH-partner **EPFL** as an additional contribution to WP5. Furthermore, the synthesis of ligand-systems for simple artificial nanopore mimicks has been started by **FZK-INT** (**M5-3** "Ligand synthesis for hexameric Fe(II) compounds (M18)").

Research work carried out in **WP 6- Biomolecular Motors on Nanostructures** has lead to different nanofabricated structures, mainly produced by **TU/d-MB**. Their optical features have been measured by total internal reflection microscopy (**M6-1** "Nanofabrication of a variety of nanostructures on coverslips (M08)"). As the electromagnetic field near the structures is poorly known, it was decided to develop a more flexible optical technique, called *Travelling Wave Tracking* (**ICG-GC**). In such a way, the nanostructures are not further used as an optical tool, but they will serve us as a three dimensional holder for the microtubules. The microtubules have been injected into the structures (**TU/d-MB**) and the activity has successfully been checked (see **M6-2** "Assembly of Microtubules on Nanostructures (M12)" and **D6-1** "Microtubules assemblies on Nanostructures (M12)").

## M18 MTRM Description of the BIOMACH Work Packages

Workpackage number <b>WP1</b>	<b>Nano-Handling</b>	Start date or starting event:			M0
Activity Type	RTD	3	5	4	10
Participant id		MPI-FKF	EPFL	ULP	AMOLF
Person-months per participant:		9	9	3	4

### Objectives

**O1** Develop **new techniques** for the handling, positioning, observation and operation of biological as well as artificial machines in the nanometer regime.

### Description of work

Temperature controlled scanning tunneling microscopy (STM), atomic force microscopy (AFM) and scanning tunneling spectroscopy (STS) are employed for nanoscale studies of molecular motors fueled with light or electrochemical energy at well-defined surfaces. Working principles of ATP-burning individual biologically relevant nano-engines are investigated using laser tweezer techniques. The time evolution of the complex molecular machines involving a large number of atoms is modeled using advanced simulation methods, notably *ab initio* molecular dynamics.

Specific goals are as follows :

- (i) concepts of molecular nanodevices exploiting metal-ligand interaction. In particular, we shall concentrate on the controlled anchoring of rotaxane (or catenane) units at surfaces either in an electrochemical environment or under ultra-high vacuum. This will allow for the synthesis of a complete rotaxane. Ultimately we work on the observation and detailed understanding of the operating of the entire species as a nanodevice.
- (ii) the study of conformational changes of molecular species which can be deliberately switched by light irradiation (e.g., exploiting photoinduced electron-transfer reactions in **LFMCs**). For the STM investigations, molecules will be designed comprising anchoring groups which allow for a specific orientation of the photosensitive group with respect to the employed substrate. Under cryogenic conditions the switching of individual species following radiation exposure is elucidated by imaging and single-molecule spectroscopy.
- (iii) study of the bacterial *Sec* system representing a model system for protein-import motors, which grab a folded protein, unfold and translocate it across a cellular membrane. Determination of the dynamics of the corresponding movements using attached micron-sized beads - serving as handles that can be manipulated by a focused laser-beam (laser tweezers) - to individual motors on one end, and to the protein on the other end.

### Deliverables

- D1-1** M24 single-molecule investigation and control of anchoring rotaxane and **LFMC** units at surfaces (report)
- D1-2** M36 modification of the vesicles and proteins involved in protein-importing molecular motors such that specific linkages to micron-sized beads can be achieved (report)

### Milestones and expected result

- M1-1** M08 identification of functionalized rotaxane and ring units grafted at surfaces
- M1-2** M16 control of **LFMCs** oriented at surfaces
- M1-3** M20 single-molecule investigation of completed devices at surface
- M1-4** M30 phenomenological description of nanodevices operating with electrochemical energy / light fuel

## Nanohandling

Catenanes and rotaxanes are the molecular architectures containing interlocked subunits that may change the relative positions under external stimulus. Grafting of such objects on a solid support represents a crucial step towards utilizing them as molecular machines in future. To understand the adsorption behaviour of catenanes or rotaxanes on solid surfaces, here we investigate the **nanohandling** of a typical building unit of catenanes, macrocycle molecule mt-33 (Figure 2a inset; the number 33 indicates the total number of atoms in the ring circumference) on a Ag(111) surface.

In order to approach milestone **M1-2** “Identification of functionalized rotaxane ring units grafted at surfaces (M08)”, the experiments were carried out in an ultra high vacuum (UHV) system. The Ag (111) surface was cleaned by repeated cycles of sputtering with 500keV Ar<sup>+</sup> - ions and subsequent annealing to ~800K. The mt-33 molecules in powder form were deposited onto the Ag (111) surface by means of organic molecule beam epitaxy (OMBE), with the crucible containing the mt-33 molecules was held at a temperature of 316°C. The Ag(111) substrate was maintained at a temperature of 300K during deposition. The prepared sample was then cooled down to 5K for STM measurements, which were performed in the constant-current mode with electrochemically etched W-tips.

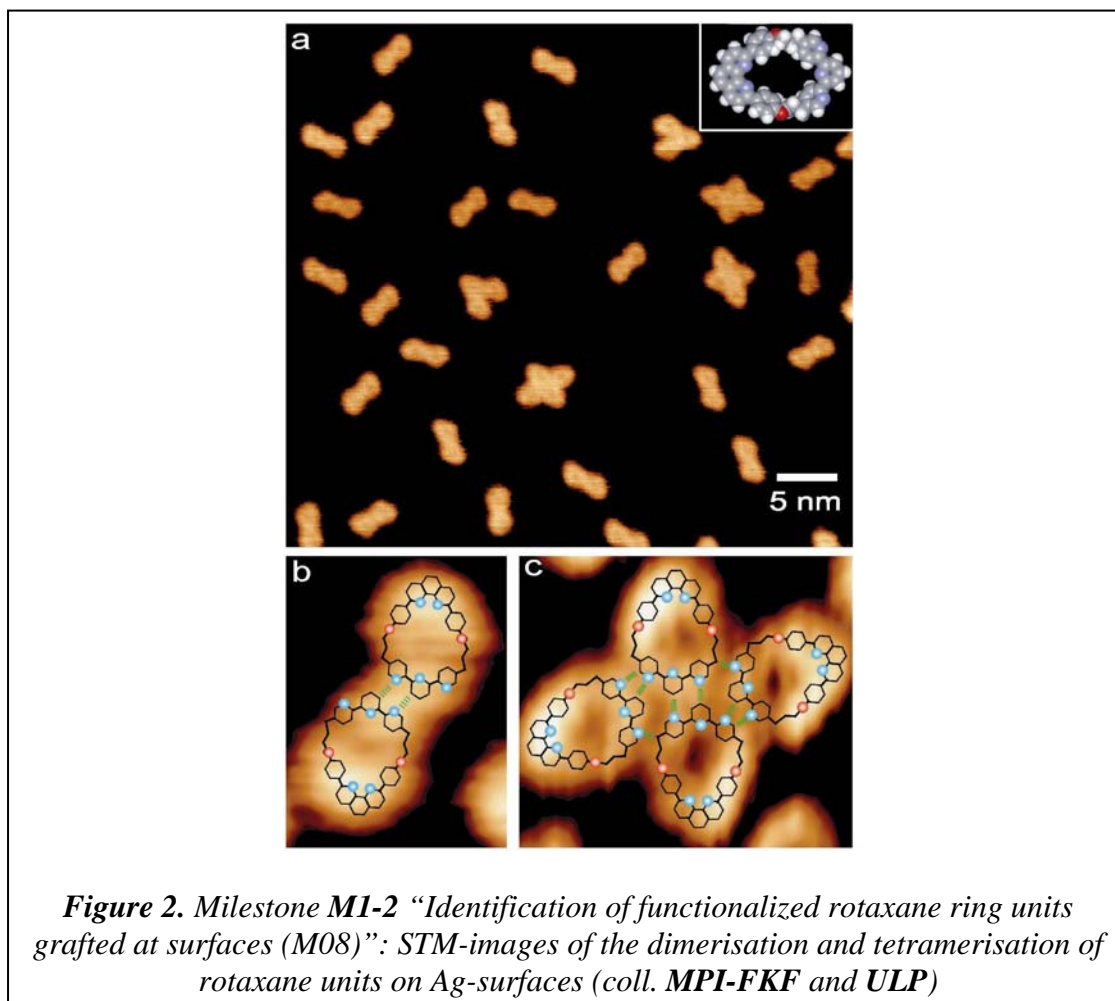
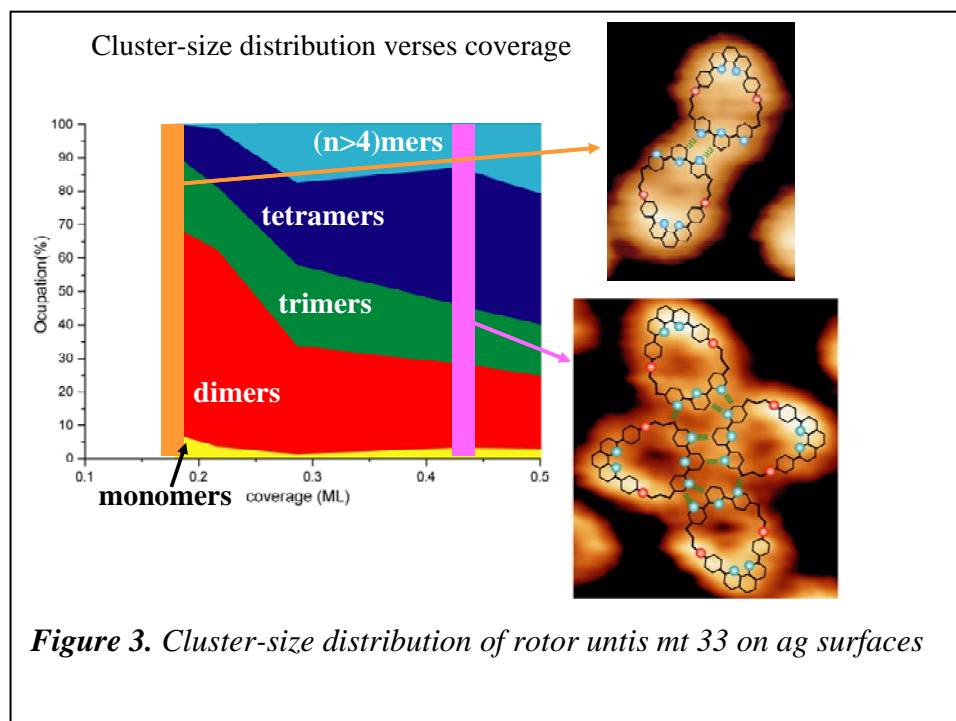




Figure 2a reproduces a typical STM topograph showing the well-defined molecular aggregates of the mt-33, wherein one can identify dimers, trimers and tetramers. In the center of each molecule there appears a dark dent, which signifies the hollow center of the ring-shaped mt-33. This observation evidences that the mt-33 molecules adsorb with their macrocycle-ring plane paralleling to the surface. In such an adsorption weak Van der Waals type forces between aromatic systems and the noble metal surface determine the mt-33 to Ag surface interactions. The weak adsorbate-surface interaction scenario is supported by the fact that while raising the surface temperature to 300K the STM only revealed some mt-33 species decorating the steps of the Ag surface, but no mt-33 aggregates observed, presumably because the mt-33 molecules are too mobile to be visualized by the STM at this temperature.

In the high-resolution data of Figure 2b and c, the asymmetric shape of the mt-33 is revealed, which consists of a broader tpy (denoted as head) part and a shaper bpy part (tail). The molecules form head-to-head arrangements for both the dimer and the tetramer. Thus the inter-molecular interactions are attributed to the hydrogen bonds between the nitrogen atoms and the aromatic carbon atoms, as proposed by the green dashed lines in Figure 2 b and c. We have found that such inter-molecular interactions create a ‘magic’ aggregation. Figure 2a displays a statistic analysis of the cluster-size distribution at five different molecular adsorption dosages, at a low density more than 50% of mt-33 molecules form dimers. With increasing of the molecular density the tetramers are gradually populated (cf. Figure 3) until they start to coalesce into larger clusters at coverage above 0.45 monolayer (1 monolayer = surface is fully covered by the mt-33 molecules). The occurrence of the ‘magic’ clusters of dimers and tetramers can be ascribed to the preferred inter-molecular hydrogen bond formation. As shown in Figure 3, in a dimer or a tetramer the head-to-head configuration efficiently saturates the hydrogen-bonding acceptor - nitrogen atoms of the tpy.



In summary, we have determined the adsorption configuration and self-assembly behavior of macrocycle molecules mt-33 at Ag(111) surface. The molecules adsorb flatly at the surface and the interactions between the molecules and the surface are weak Van der Waals forces. At low temperatures, the molecules tend to aggregate as dimers and tetramers via the inter-molecular hydrogen bonds.

The milestone **M1-2** “Control of LPMC’s oriented at surface (M16)” has been achieved by the close collaboration between **MPI-FKF** and **FZK-INT**; further scientific details are described in WP 4 under the strongly overlaying milestone **M4-3**. However, in preparation of the experiments with light-driven molecular motors, a laser system has been installed at an ultra-high vacuum chamber in order to study light-driven molecular motions under the well-defined conditions. The laser source is a Helium Cadmium (HeCd) laser manufactured by Melles Griot Laser Group (USA), which outputs two wavelengths of 325 nm and 442 nm. The laser power is 10mW (325 nm) and 25mW (442 nm). As shown in the figure below, the laser light is guided by a fiber optics into the vacuum system. The vacuum linear feedthrough setup is able to manipulate the end of the optic fiber towards the tip-sample junction of a scanning tunneling microscope (STM) at a distance of 20 mm. The design allows shining the laser light at the sample surface during the STM measurement. The vacuum system is equipped by standard facilities to prepare clean surfaces and bring interested molecules on the surfaces by thermal sublimation. The sample temperature is controlled by liquid nitrogen or liquid helium cooling and thermal heating in a range of 30 K to 500 K.

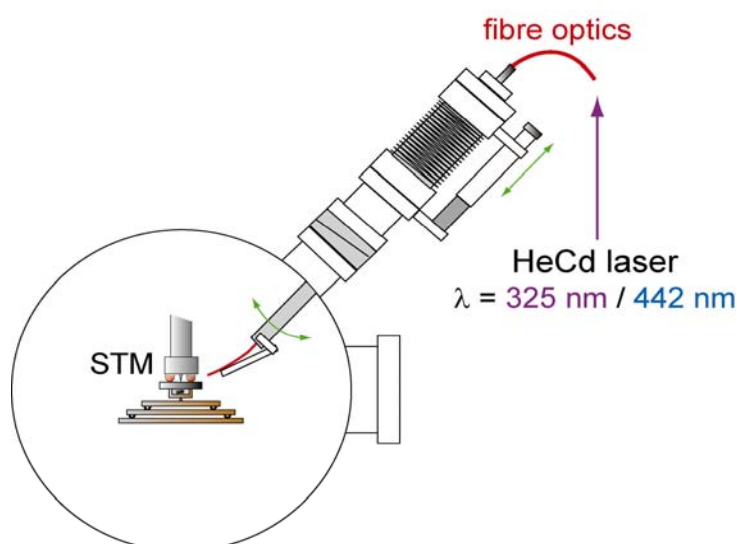


**Figure 4.** As contribution to **M1-2**, an UHV-Laser-STM system was designed by BIOMACH partner **MPI-FKF**

## Conclusion

Milestones **M1-1** and **M1-2** were achieved by a three-centre collaboration between **FZK-INT**, **ULP** and **MPI-FKF** and, additionally, a technological platform in preparation of the experiments with light-induced molecular motions in WP 4 was designed. The obtained results represent the base for the preparation in-time of **D1-1** “Single molecule investigation and control of anchoring rotaxane- and LPMC units (M24)”.

Workpackage number	Self-Assembly	Start date or starting event:			M0
WP 2					
Activity Type	RTD	6	3	8	9
Participant id		EPFL	Tu/e	MPI-FKF	FZK-INT
Person-months per participant		12	9	3	3

### Objectives

**O2** Investigate new self-assembly strategies for the *in-situ* build-up of artificial motors from separate components.

### Description of work

The work in this work package consists of two independent lines of research. The first line focuses on the synthesis of novel scaffolds that give compatible Au-anchored receptor sites for the rotary motors. This will be performed in close collaboration with the other work packages in which both the artificial (rotaxane/catenane) as well natural rotary motors are synthesized and studied. The second line of research focuses on the further elaboration of the chiral an/or semi-conducting self-assembling cylindrical stacks on the one hand and the derivatisation of the rotary motors in such a way that they can intercalate into the cylindrical stacks. This work requires synthesis, nano-processing of the self-assembly as well as detailed characterization of the objects obtained for and after the intercalation of the rotary motors. The work of semi-conducting self-assembled polymers is part of an ongoing collaborative research project with Philips Research towards novel organic devices for electronics. The hydrogen-bonded polymeric structures are the main activity of a new start-up company Suprapolix focus on application of specific self-assembled functional polymers. The Eindhoven group has a strong collaboration with this new company.

### Deliverables

- D2-1** M-24 Self-assembled chiral stacks including intercalated rotary motors included (report)  
**D2-2** M-36 Self-assembled semi-conducting polymers including intercalated rotary motors included (report)

### Milestones and expected results

- M2-1** M-12 Synthesis of the scaffolds for the Au-anchoring, both for the inert environment as well as the functional receptor site (hydrogen bond and streptavidin)  
**M2-2** M-12 Synthesis of the modified rotary rotor and its self-assembly by hydrogen bonds and biotin  
**M2-3** M-20 Synthesis of chiral scaffold  
**M2-4** M-24 Synthesis of semi-conducting scaffold  
**M2-5** M-30 Self-assembly of both chiral and semi-conducting scaffolds  
**M2-6** M-36 Analysis of the nano-processed structures.

## Self-Assembly

The self-assembly of functionalized molecules in two-dimensions (2D) on solid surfaces provides access to several candidates for potential applications such as organic network templates, molecular mechanic or electronic devices. The comprehension how the molecular bricks self-arrange into a monolayer becomes so a key step in the construction of molecular devices. In general, the structure of organic monolayers on solid surfaces strongly depends on the size and symmetry of the molecule and the lattice of the underlying substrate. Thereby, scanning tunnelling microscopy provides a powerful tool for addressing the structure of the organic monolayer on solid surfaces with atomic and submolecular accuracy. An increasing number of organic molecules on different solid surfaces, such as Au and HOPG have been investigated by STM techniques and the built-up of molecular scaffolds for the step-by-step hierarchical built-up of mechanical devices is being investigated within **WP 2 – Self-Assembly**.

In order to obtain milestone **M2-1** “Synthesis of the scaffolds for the Au anchoring”, the BIOMACH partner **FZK-INT** has synthesized the molecule ExTMA (see Figure 5). This molecule was sublimated to Ag-surface (instead to the more sticky Au) to fabricate 2-dimensional networks containing extremely large voids. The diameter of the open voids is as large as 3 nm, which is suitable to accommodate various catenane or rotaxane molecules. Because of the perfect long-range ordering of the voids, one may use this surface as a template to organize the catenane or rotaxane molecules as well-defined arrays at a surface.

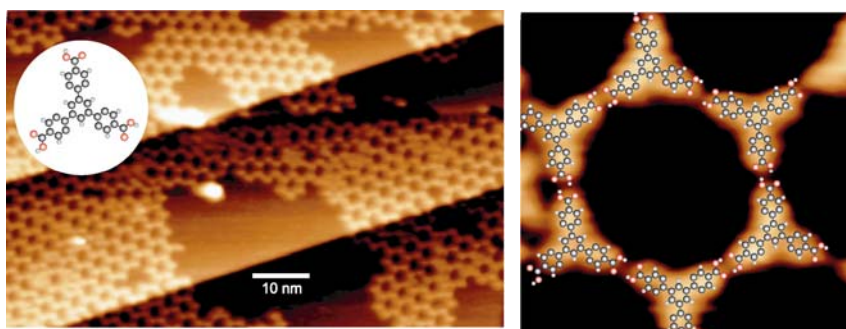


**Figure 5.** Milestone **M2-1** “Synthesis of the scaffolds for the Au anchoring (M12)”: A 2D honeycomb network from the self-assembly of ExTMA on an Ag surface exhibiting large voids for hosting rotaxane units. (Collaboration **FZK-INT** and **MPI-FKF**)

In order to approach milestone **M2-2** “Synthesis of the modified rotary rotors and its self-assembly (M12)” and to avoid the in WP1 described dimer- and tetramerisation of the rotaxan units at surfaces (*vide supra*), the BIOMACH partners **FZK-INT**, **ULP** and **MPI-FZK** were able to confine monomeric catenane or rotaxane molecules into in these voids. In detail, the tricarboxylic acid ExTMA, which has been synthesized by the **FZK-INT**, was used as the starting unit. The molecules have been successfully sublimated in vacuum onto a Ag(111) surface and self-assemble as 2D honeycomb network architectures as shown in Figure 5 left. Figure 5 right reveals that the intermolecular interactions are hydrogen bonds between the carboxylic endgroups.

To realize molecular motion of surface-supported catenanes and rotaxanes, it is essential to adsorb the molecules individually at a surface, i.e., each molecule is free of coupling to the neighboring species. Following our previous success of preparing ‘magic’ clusters of macrocycle molecules mt-33 at a Ag(111) surface, here we report our efforts to position single mt-33 molecules at the surface. Due to the weak interactions between the mt-33 and the Ag surface, the mt-33 molecules are highly mobile and readily forming clusters, i.e., no single-molecule adsorption. To overcome this obstacle we proposed a route that is schematically shown in Figure 6. First nanometer size cavities are grown at the surface. Then at the second step, the mt-33 molecules are deposited, wherein the single molecules are confined in the nanometer-size cavities. Thus, a rotaxane unit (synthesized by **ULP**) was cosublimed onto the honey comb network (**FZK-INT**) in such way, that monomeric (instead the before observed higher multimers) species have been attached to the bare metallic surface within the voids (experiment carried out by **MPI-FKF**).

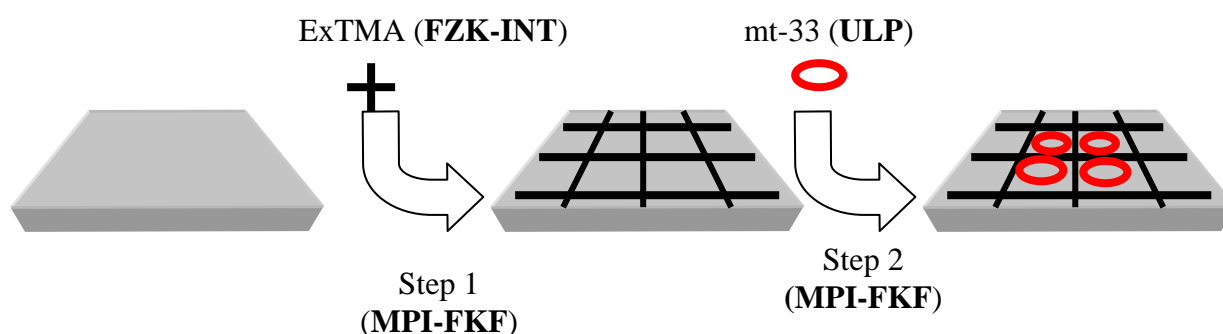


**Figure 6.** Schematic representation of the realisation of **M2-2**: Stepwise built-up of a scaffold-rotor unit on a Ag-surface

In detail, the nanometer cavities have been prepared by the self-assembly of ExTMA (4, 4', 4''-benzene-1,3,5-triyl-tri-benzoic acid) molecules at the clean Ag(111) surface. The ExTMA molecules were sublimated by means of organic molecule beam epitaxy (OMBE), with the crucible was held at a temperature of 270°C. The Ag(111) substrate was maintained at a temperature of 280K during deposition. The prepared sample was then cooled down to 150K for mt-33 deposition. Then the sample was transferred into the 5K-STM for measurements.

Figure 7a reproduces a typical STM topograph showing the self-assembled honeycomb structures stabilized by hydrogen bonds between the carboxylic endgroups. The structure contains an array of cavities of 2.95 nm diameter, which represent an idea host to accommodate single mt-33 molecules. The triangular object marked by the dashed circle is an ExTMA molecule confined in a honeycomb cavity. After deposition of the mt-33 molecules, STM shows that many honeycomb cavities hold larger species that have a hollow center, as highlighted by the solid ellipse in Figure 7b. The size, shape and the hollow-center appearance of these objects clearly prove they are mt-33 molecules. Because of the size matching, only single species may be accommodated in on cavity. As comparison the dashed circle points a confined ExTMA molecule. So we have successfully grafted individual mt-33 molecules at the surface by the proposed route! Based on the STM data, the inset in Figure 7b displays a model showing a single mt-33 molecule in the honeycomb cavity. Furthermore the confined mt-33 molecules compose a regular single-molecular array following the periodic arrangement of the honeycomb cavities.

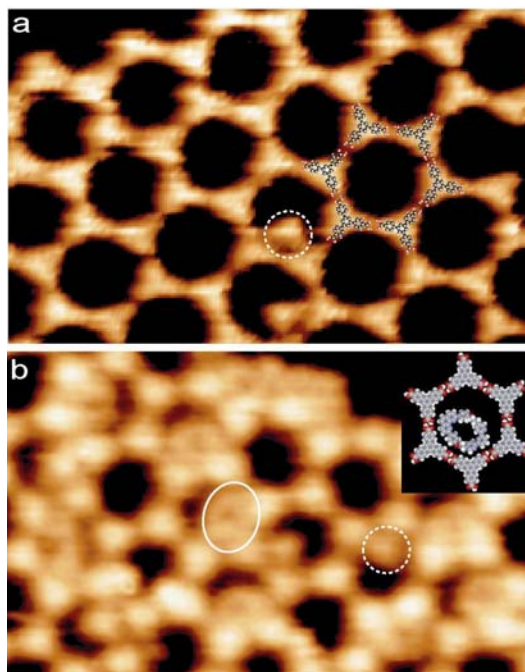


**Figure 7.** Milestone **M2-2** “Synthesis of the modified rotary rotors and its self-assembly (M12)”: Representation of *mt-33* within the void of the scaffold formed by self-assembly of *Ex-TMA*

Additionally, the BIOMACH partner **EPFL** has been studying alternative self-assembly techniques based on Hydrogen-bonding and metal coordination effects, which might be also used in the attempt to assemble molecular motors directly on the surface.

Complementary to the above represented results on surfaces, the BIOMACH partner **Tu/e** is studying self-assembly events in solution. This work will lead to milestones **M2-3** “Synthesis of a chiral scaffold (M20)” and **M2-4** “Synthesis of semi-conducting scaffolds (M24). Later on, the two research lines in WP 2, self-assembly on surfaces and in solution, will be merged to a single scientific effort.

## Conclusion

The milestones **M2-1** and **M2-2** (joint with M4-3) have been achieved and work on milestones **M2-3** and **M2-4** has been started by **Tu/e**. Although representing only first steps, the results support strongly the new approach to self-assemble molecular motors from their components either on surface or in solution.



<b>Workpackage number</b> <b>WP 3</b>	<b>Electro-Engines</b>	<b>Start date or starting event:</b>			M0
<b>Activity Type</b> <b>Participant id</b>	<b>RTD</b>	<b>9</b> ULP	<b>2</b> FZK-INT	<b>5</b> MPI-FKF	<b>6</b> CIAM
<b>Person-months per participant:</b>		12	3	9	6

**Objectives**

**O3** Design, synthesize and handle the **first artificial ATPase**-like molecular rotators.

**Description of work**

Synthesis of a rotaxane able to work as an oscillatory machine. The rotor (a macrocyclic ring) and the stator (a molecular thread) are linked together via a transition metal. The ring incorporates two different coordinating sites, a bi- and terdentate site. The thread incorporates one bidentate site. The position of the ring on the axis will be determined by the oxidation state of the metal, which can be electrochemically monitored. A thick filament ended by a voluminous moiety, such as a porphyrin, is attached to the ring. The axis of the rotaxane is ended at each end by functionalities which will allow the attachment of the machine onto a gold surfaces, in form of self-assembled monolayers. The operation of the machine will be triggered the potential of the host surface. The spinning of the filament, i.e. the rotor, will be investigated by scanning probe microscopy or by optical methods.

**Deliverables**

**D3-1** M12 Catenanes and rotaxanes units grafted on a metal surface (report)  
**D3-3** M36 Monolayers of rotaxanes working as molecular devices (report)

**Milestones and expected results**

**M3-1** M06 Synthesis of a switchable rotaxane units bearing the appropriate functional group for grafting.  
**M3-2** M12 Grafting of the rotaxane at a surface and study of the electrochemically induced rotation motion.  
**M3-3** M30 Synthesis of the bistable rotaxane with a long filament attached on the ring

## Electroengines

The objective of **WP3** for the 18 months of the project was the grafting of catenane and rotaxane units on a metal surface.

### a) catenanes

The first approach consists in vaporizing on a metal surface the ligands and then to introduce a metal cation ( $\text{Cu}^+$ ). The motions of the ligands, induced by changing the oxidation state of the copper atom, will be examined by STM techniques. This project requires the synthesis of the macrocycles shown in Figure 8. High vacuum sublimation and subsequent studies on the surface by STM are developed in paragraph 2.

### b) rotaxanes

The second approach consist in preparing pseudo-rotaxanes and rotaxanes followed by their grafting on an electrode surface. The analysis of their electrochemical behavior should permit to establish the rate of the motions on the surface as well as in solution and to determine important structural parameters. This approach is developed on paragraph 1 (synthesis and electrochemical behavior in solution and on electrode surface). The molecules prepared are shown on Figure 10 and Figure 11.

## Synthesis, solution studies and surface deposition (ULP)

**M3-1 “Synthesis of a switchable rotaxane bearing functional groups fro grafting (M06)” and**

**M3-2 “Grafting of the rotaxane at the surface and study of the electrochemically induced rotation (M12)”**

### Introduction and synthesis

It is important to visualise the dap chelate and macrocycles m-30 and mt-33 (Figure 8; the numbers 30 and 33 indicate the total number of atoms in the rings circumference) if one wants to observe large amplitude molecular motions in copper-complexed catenanes containing these molecular fragments as components. The compounds have been synthesized and sent to Dr. Nian Lin (**MPI-FKF**).

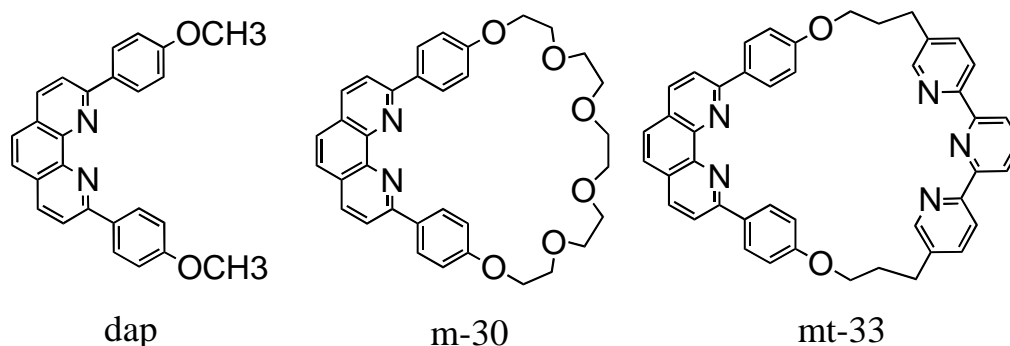


**Figure 8.** Chemical structures of 2,9-dianisyl-1,10-phenanthroline and macrocyclic ligands

The next step will be to observe, on the surface, two interlocking rings as represented in Figure 9 (catenanes **1** and **2**). In a subsequent step, the introduction of copper(I) within these complexing molecules will allow to visualise the motion of the rings, the free molecules rearranging so as to reach the equilibrium position corresponding to the formation of the



copper(I) complexes. An electrochemical signal ( $\text{Cu}^{\text{II}}/\text{Cu}^{\text{I}}$ ) will also be used to trigger a large amplitude motion.

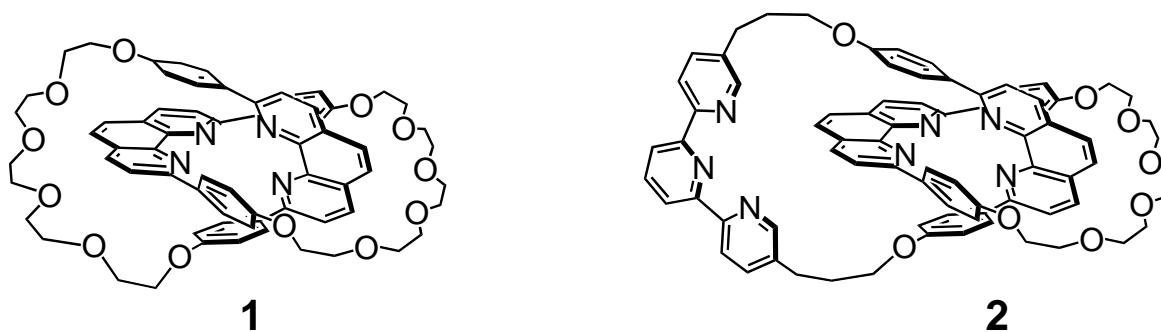


**Figure 9.** Chemical structures of the catenanes cat-30 (1) and cat-mt-33(2).

As far as rotaxanes are concerned, the switchable rotaxane **3**, bearing the appropriate functional group for grafting, has been prepared. **3** of Figure 3a (“pre-rotaxane”) containing :

(1) a bipy unit, which is threaded inside the ring (bipy = 2,2'-bipyridine). This “thread” will constitute the fixed part of the future rotary motor.

(2) a ring, which incorporates both a dpp motif and a terpy fragment (dpp = 2,9-diphenyl-1,10-phenanthroline ; terpy : 2,2',6',2''-terpyridine ; dpp is a bidentate chelate whereas terpy is a tridentate chelate).

(3) a sulfur-containing function (thioacetate, thiol, thioether or disulfide), allowing adsorption and grafting of the molecule on a gold surface (Figure 10a).

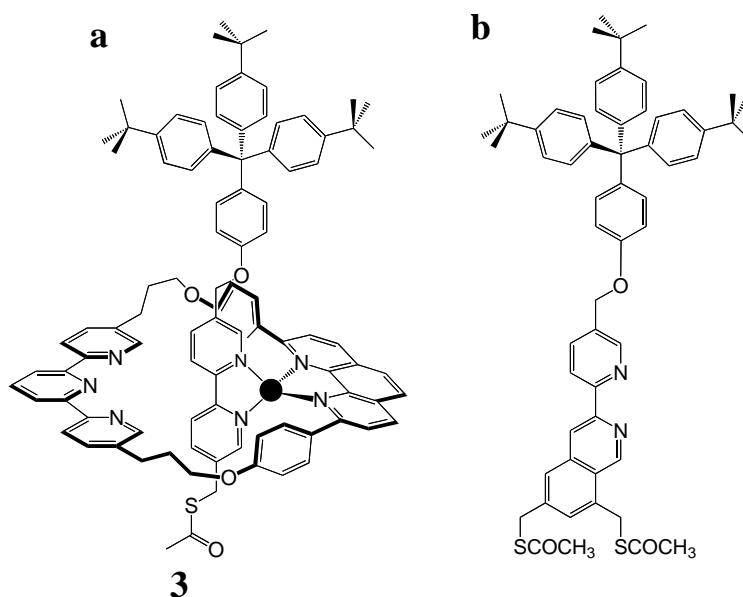


**Figure 10.** chemical structures of the a copper rotaxane and of a new ligand, which will allow perfect control of the pirouetting motion; compound **3** has been made by Dr Hanss and Dr Collin.

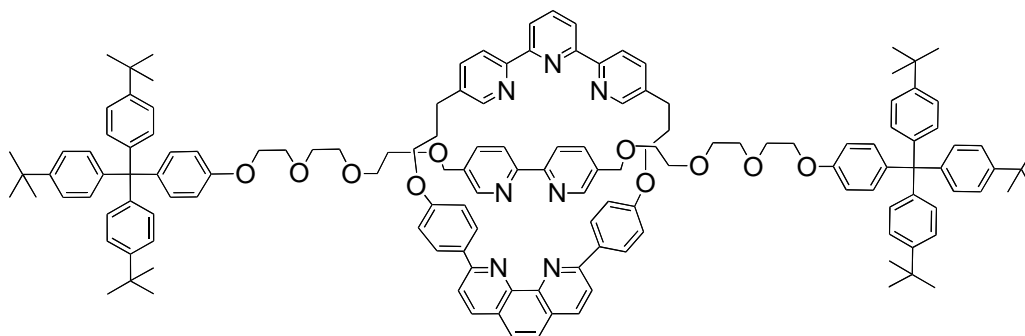
Stepwise synthesis allowed us to obtain the pseudo-rotaxane **3** in reasonably good yield (31%). A detailed  $^1\text{H}$ -NMR study of compound **3** shows that the threading reaction of the bipy-containing “filament” is quantitative. In order to immobilize a pre-rotaxane and to generate a surface-deposited rotaxane attached to the surface in a rigid way, we have designed a new molecular thread, with a novel bidentate chelate consisting of a pyridine nucleus and a disubstituted isoquinoline moiety (Figure 10b) The chemical structure of the thread, with its two anchoring points (S-containing functions), is such that *it will prevent the axial stator from rotating*. This synthetic work is now pursued in our group.

### Electrochemical studies in solution and deposition on a gold surface

Cyclic voltammetry measurements show that, in solution, the present system is set in motion particularly efficiently by an electrochemical signal. It is the fastest copper-complexed rotaxane or catenane to rearrange, among all the compounds made and investigated in our group.

**3** could be deposited on a gold surface. The reaction time required for complete adsorption of the pre-rotaxane on a gold bead is around one week. By electrochemistry, it could be demonstrated that the movements are very slow on the surface, in spite of the efficiency of the system in solution. In order to circumvent this difficulty, a possible solution would be to “dilute” the dynamic molecular system on the gold surface by proceeding to co-adsorption of thioalcanes molecules such as HS-(CH<sub>2</sub>)<sub>n</sub>-CH<sub>3</sub> (n = 17) at the same time as the pseudo-rotaxane **3**. In such a way, the ring to be set in motion should be sufficiently remote from the gold surface to be able to move readily, similarly to what was observed in solution.

A rotaxane with a dpp-incorporating axle and the macrocycle mt-33 has been synthesized a few years ago, but the response time of the compound was relatively long (seconds). Since the presence of voluminous stoppers close to the copper centre is likely to slow down any reorganisation process occurring within the metal coordination sphere, we decided to make a much less sterically hindered system, with no substituents close to the metal and with long connectors between the copper complex core and the stoppers. A new synthetic route had to be planned and realised, which will not be included in this report. The free rotaxane of Figure 11 could be prepared following a multistep procedure.



free rotaxane **4**

*Figure 11: chemical structure of a rotaxane with two remote stoppers of the electroactive site; this compound has been prepared by Dr L  tinois under the supervision of Dr Collin.*

The electrochemical behaviour of **Cu.4** has been investigated in CH<sub>3</sub>CN solution by cyclic voltammetry at a platinum electrode. Starting from the ligand **4** and the corresponding stoichiometric amount of Cu(CH<sub>3</sub>CN)<sub>4</sub><sup>+</sup>, it is possible to generate in situ and quantitatively the copper(I) rotaxane **Cu.4**. Preliminary results indicate that the motion of the ligands around the copper(II) centre, from the tetra-coordinated form to the penta-coordinated state, is very fast even at – 40 °C. These experiments seem to confirm that destabilisation of the copper(I) complex could be achieved both by removing the substituents in alpha position to the nitrogen atoms of the 2,2'-bipyridine ligand and by increasing the distance between the stopper units and the coordination site. These two parameters appear to be determining and will allow us to optimize the design of future fast-moving molecular machines.

## Conclusion

The results obtained at the end of the first year of the contract as far as the Deliverable **D3-1** is concerned show that the objectives have been achieved. Indeed the two milestones **M3-1** and **M3-2** have been realized:

- A copper rotaxane, designed to move by changing the oxidation state of the metal and functionalized by a thioacetate group, has been successfully synthesized (**ULP**).

- This copper rotaxane has been grafted on an Au surface and its electrochemical behaviour has been investigated (**ULP**).

Additionally to these two essential steps we have undertaken the grafting of macrocycles and catenanes by high vacuum sublimation. This goal has been successfully achieved for the molecules dap, m30 and mt-33 as demonstrated by the STM images obtained **MPI-FKF**. This group has also undertaken together with **FZK-INT** the elaboration and study of two-dimensional honeycomb network suitable to accommodate catenanes (see WP 2).

The analysis of the whole results allows us to define the main research axis for the next months. In fact, we need better functionalizing group in order to obtain an easier grafting on Au surface. We also need to synthesize a pseudo-rotaxane in which the stoppers are remote from the electroactive site. The synthesis of catenanes as described in Figure 2 and their STM studies will also be pursued.

Workpackage number <b>WP 4</b>	<b>Photochemical Devices</b>	<b>Start date or starting event:</b>		M0
<b>Activity Type</b> <b>RTD</b>	<b>2</b>	7	1	9
<b>Participant id</b>	<b>CIAM</b>	ETH	FZK-INT	ULP
<b>Person-months per participant:</b>	<b>15</b>	21	3	3

**Objectives**

**O4** Integrate appropriate Light-Fueled Molecular Components (LFMC's) into nano-motors as **alternative fueling** concept.

**Description of work**

The research groups of **WP4**, taking advantage of a long-term background in inorganic and organic spectroscopy, photochemistry and electrochemistry, have gained considerable expertise in the design and characterization of supramolecular species under the photo-physical, photochemical and electrochemical viewpoint, with the main objective of realizing prototypes of molecular-level devices and machines.

The main tasks of the **WP4** in the frame of the Network are:

- design of molecular components and supramolecular systems upon evaluation of the possible light-induced processes and electron-transfer reactions that can occur in such compounds.
- photo-physical, photochemical and electrochemical characterization.
- integrate the use of molecular dynamics simulations into the design of such devices by evaluating the microscopic mechanism of processes prior to the synthesis of devices.

**Deliverables**

**D 4-1** M12 Final Design of a Light-Fueled Molecular Component (LFMC) (report)

**D 4-2** M18 Computational treatment of light-induced rotary movements in LFMC's (report)

**D 4-2** M36 Operation of LFMC-incorporating photodriven molecular machines (report)

**Milestones and expected results**

**M 4-1** M06 Planning and synthesis of a LFMC

**M 4-2** M12 Photo-physical characterization of LFMC's in solution

**M 4-3** M16 Self-assembly of LFMC's on surfaces (WP2)

**M 4-4** M24 Incorporation of LFMC's into biological-type environments (WP2 and WP6)

**M 4-5** M30 Study of the operation LFMC-driven molecular devices and machines (WP1)

## Photochemical Devices

### Introduction

The task of molecular motors is to convert a certain form of energy (chemical, electrochemical, photochemical) into mechanical work that can be subsequently used to achieve a function within molecular machines. Therefore molecular motors, like macroscopic ones, operate by consuming energy.

An obvious way to supply energy to a chemical system is through an exergonic chemical reaction, as happens in our body for the motor proteins myosin and kinesin that are driven by the free energy provided by ATP hydrolysis. If an artificial molecular motor has to work by inputs of chemical energy, it will need addition of fresh reactants (fuels) at any step of its working cycle, with the concomitant formation of waste products that can compromise the operation of the device unless they are removed from the system. The need to remove waste products, indeed achieved magnificently in natural systems, introduces noticeable limitations in the design and construction of artificial molecular motors based on chemical fuel inputs.

Light can cause the occurrence of *endergonic* and *reversible* reactions, and therefore photons are suitable energy inputs to power artificial molecular devices. In such a context, light stimulation has several important advantages compared to other energy inputs:

- 1) it is very easy to achieve (by means of lamps or lasers, or from the sun);
- 2) the amount of energy conferred to the chemical systems can be precisely controlled by adjusting the radiation's wavelength;
- 3) it can be switched on and off easily and rapidly;
- 4) it can be performed with high spatial (down to nm level with near-field techniques) and temporal control (down to fs time domain);
- 5) there is no need to "touch" or to "wire" the molecules to the energy source;
- 6) photons can also be used to read the state of the system: by means of luminescence spectroscopy, for instance, detection can be made at the single molecule level;
- 7) the formation of waste products can be prevented by using "clean" photochemical reactions;

Another important feature of molecular motors is their capability to exhibit an *autonomous* behavior; that is, to keep operating, in a constant environment, as long as the energy source is available. Natural motors are autonomous, but the vast majority of the artificial molecular motors reported so far are *not autonomous* since, after the mechanical movement induced by a given input, they need another, opposite input to reset. As it will be shown later on, by exploiting light-induced processes in appropriately designed systems it is possible to make artificial molecular motors showing autonomous behavior.

Two kind of light-induced processes are particularly suitable for fueling artificial molecular motors: photoinduced electron-transfer and photoisomerization reactions.

In the first case, photoinduced electron transfer processes involving a "light-fueled molecular component" are employed to change the electronic distribution within a carefully designed supramolecular system. Such a change then causes large amplitude motions of the molecular components, leading to conversion of a fraction of the photon's energy into chemical free energy that is available to do mechanical work.

In the second case, the structural change associated with light excitation of a photoisomerizable molecule are used to obtain large amplitude motions. Suitable systems in this regard are derivatives of azobenzene, stilbene and other photoisomerizable groups (diarylethenes, spiropyrans, etc.).

## Molecular motors based on photoinduced electron-transfer processes

### M4-1 “Planning and Synthesis of a LFMC (M06)”

Molecular motors based on this approach must contain two basic devices:

- a light-fueled device, in charge of absorbing the photon and processing its energy by transferring electrons to other components of the system;
- a mechanical switching device, which contains the molecular parts that can be potentially moved.

Of course these two devices must be structurally and functionally integrated with each other such that the light-fueled device can power the molecular motions in the mechanical switching device. The requirements that the light-fueled component must fulfil to carry out its task, namely:

- 1) be capable of absorbing light with high efficiency in the desired wavelength range
- 2) possess a long lived electronically excited state with suitable redox properties
- 3) exhibit convenient ground- and excited-state spectroscopic signatures, in order to facilitate the observation of the occurring processes
- 4) be easy to connect with other molecular components via covalent linking or self-assembly
- 5) show chemical stability in the conditions of operation

have been clearly identified as the first milestone.

After investigating the photophysical and electrochemical properties of several compounds in solution, the CIAM group found that good candidates for the role of light-fueled device are the Ruthenium(II) complexes of the polypyridine family, like  $[\text{Ru}(\text{bpy})_3]^{2+}$  (bpy=2,2'-bipyridine).

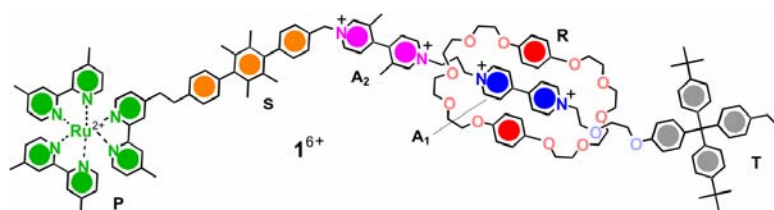
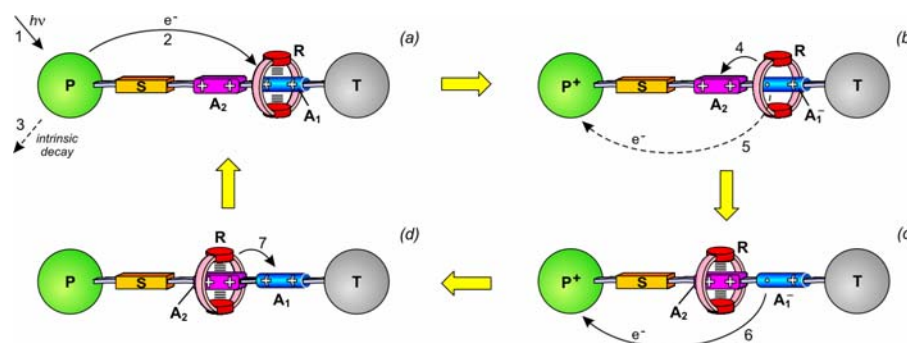


**Figure 12.** Structure formula of the rotaxane  $1^{6+}$

Therefore, in collaboration with the group of prof. Fraser Stoddart at the University of California, Los Angeles, **CIAM** came up with the design and synthesis of the rotaxane  $1^{6+}$  (Figure 12). Shuttling of the ring for approximately 1.3 nm between the two stations  $A_1$  and  $A_2$  could be obtained by a purely intramolecular mechanism based on a sequence of electron-transfer and nuclear processes (Figure 13). The operation of this nanomotor, which is autonomous and is powered exclusively by visible light, takes place in four strokes: destabilization of the stable co-conformation, displacement of the ring, electronic reset, and nuclear reset.

**Figure 13.** Mechanism of the photochemically driven ring shuttling in rotaxane  $1^{6+}$ .



## M2-2 “Photophysical Characterisation of LFMC’s in solution (M12)”

The crucial point for the mechanism is indeed the favorable competition between ring displacement (process 4) and back electron transfer (process 5). It was found that the system works in ambient conditions, and converts ~10% of the photon energy into mechanical movement.

The efficiency of this motor is low, particularly in comparison with the performance of natural motors. However, the operation of the system is based on the challenge that a complex nuclear motion can compete with an electron transfer process. The rotaxane design can in principle be improved upon, thanks to the experience gathered in this research. Several directions of future work in this regard have been illustrated. All this results were concluded in detail in **D4-1** “ Final Desig of a LFMC (M12)”.

In order to provide a better understanding of the atomic mechanisms which rule the behavior of a molecular nanomotor, the **ETH** group performed calculations on the rotaxane **1**<sup>6+</sup> (Figure 12). More specifically, the goal of **ETH** is to compute the energy barriers related to this process and to understand at the atomic level how the movement occurs. The tools that were used are all atom molecular dynamics (MD) simulations and the metadynamics.

The key observations are the following:

- At equilibrium at least one  $\text{PF}_6^-$  anion remains stuck to the rotaxane, whichever the starting configuration. This contrasts with the common belief that in polar solvents the counterions are well separated from the cationic rotaxane. However, since it could not be excluded that this is not an artifact related to the small size of the simulation cell, in the metadynamics runs the counterions were forced to remain far apart from the rotaxane, postponing a more careful analysis of this point to a later time. It is worth noting that a specific effect of the counterions on the shuttling dynamics in a related rotaxane has recently been observed for the first time by the **CIAM** group.
  - Starting from different initial configurations the presence of two deep basins of attraction, corresponding to the ring encircling the two stations, could be identified. Many metadynamics runs were carried out using different numbers and combinations of collective variables for the reduced configuration. At least three are necessary to correctly reproduce the physics of the system: the best choice appeared to be the position of the ring along the dumbbell and the number of hydrogen bonds formed with the first and second station, respectively. The barrier for the ring moving from the **A**<sub>1</sub><sup>+</sup> station to the **A**<sub>2</sub> station was determined to be 8 kcal/mole, while it is about 13 kcal/mol for the reverse process. Both value are slightly smaller than those observed by the **CIAM** group (12 and 14 kcal/mole, respectively), but it should be recalled that the estimated accuracy of our values is of about 1.5 kcal/mole and that the role of the counterions is still under investigation.
  - Many smooth shuttling processes were observed in the calculations and the atomic mechanism can be sketched in three steps (Figure 14). First, the hydrogen bonds between the ring and the hosting station are broken, with the ring assuming an almost orthogonal position with respect to the dumbbell. Second, the ring shuttles towards the other station. Third, the ring rotates and establishes the hydrogen bonds with the new hosting station.
- All this results were conclude din detail in **D4-2** “ Computational treatment of light-induced rotary movements in LFMC’s (M18)”.

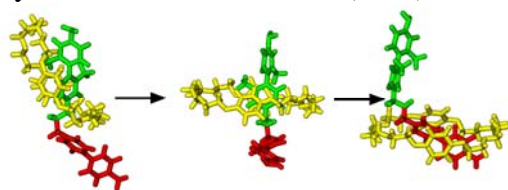


**Figure 14.** Movement of the crown ether (yellow) from one green station to the red one. For clarity the solvent, the counter-ions and the rest of the rotaxane are not displayed.



### Molecular motors based on a photoisomerization reaction in near-surface conditions M4-3 “Self-assembly of LFMC’s on surfaces (M16)” together with M 1-2; WP 1

Photoisomerization reactions, like the *trans-cis* photoisomerization around the N=N bond in azobenzene derivatives (Figure 15), represent a class of photochemical processes that could be profitably used to construct light-powered molecular machines because they are fast, reversible, and gives rise to large geometrical changes of the molecule. In this case the same unit (azobenzene) plays the roles of both the LFMC and the “movable” part.

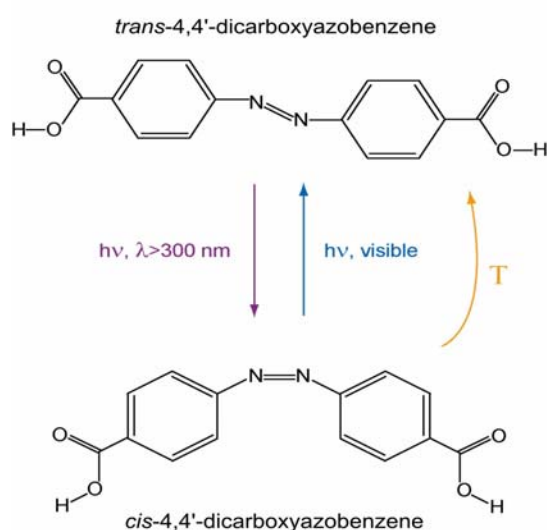


**Figure 15.** The *trans-cis* photoisomerization of the LFMC 4,4'-dicarboxyazobenzene.

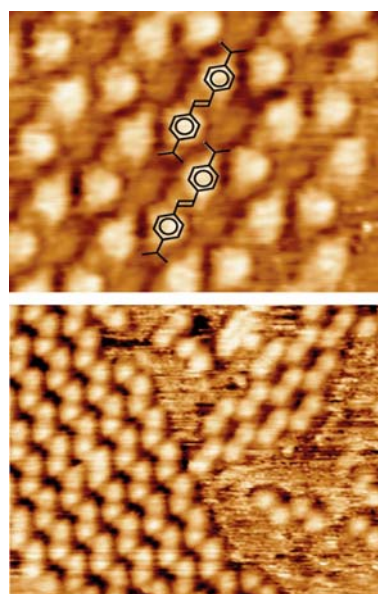


**Figure 16.** (a) STM images of a monolayer of *trans*-4,4'-dicarboxyazobenzene on Cu(100), showing the formation of *trans*-domains.

While photoisomerization of these compounds is well known<sup>Fehler! Textmarke nicht definiert.</sup> in solution and in the bulk, experiments must be performed to explore the photoisomerization within a monolayer on a solid surface. For this purpose the **FZK-INT** group synthesized compound 4,4'-dicarboxyazobenzene (Figure 15) following a modified literature protocol. In a subsequent step, the compound was sublimed within a UHV-chamber onto a Cu(100) surface, where the monolayer formation, driven by hydrogen bonding or achieved through metal-ligand interactions, was followed by STM in collaboration with **MPI-FKF** (Figure 16). In the first case, only formation of *trans*-domain could be observed. The next step is to see if the dicarboxyazobenzene molecules can be photoisomerized on the surface and, in case, whether *cis*-domain are obtained. Irradiation experiments in collaboration between **FZK-INT** and **MPI-FKF** are ongoing as scheduled.



## Conclusion

The objective of this WP is to integrate light-fueled molecular components (LFMC's) into artificial nanomotors as an alternative fueling strategy. This objective was approached by investigating two types of systems.

1) Shuttling of a molecular ring along a dumbbell component in a rotaxane caused by a photoinduced sequence of electron-transfer processes. The rotaxane contains a LFMC in the form of a Ru(II) polypyridine complex that is distinct from the mechanical switching part. Detailed spectroscopic investigations allowed **CIAM** to show that the investigated rotaxane behaves as an autonomous nanomotor driven by visible light in solution, albeit with a low efficiency. Computational simulations of the system carried out by **ETH** have started to unravel the mechanism of the shuttling process, and are expected to be crucial for the design of novel prototypes with improved performance. The work is proceeding in close cooperation between **CIAM** and **ETH**.

2) *Trans-cis* photoisomerization of an azobenzene derivative on a metal surface. The experiments, performed by **FZK-INT** in connection with **MPI-FKF**, showed that the azobenzene species can be deposited as a monolayer onto a Cu(100) surface by sublimation under UHV conditions. The subnanometer-scale STM topographic studies of the surface revealed that domains of the *trans*-isomer are formed. Photoisomerization studies on such molecules under near-surface conditions are underway in cooperation with **MPI-FKF** (see WP 1).

In summary, the results expected for the first two milestones have satisfactorily been achieved, and the first deliverable was regularly delivered. The exchange of information among the partners of the WP is very good, and there is a high degree of interaction between **CIAM** and **ETH**. Efforts will be made to strengthen collaboration between partners it in the future months.

<b>Workpackage number</b> WP5	<b>Nanopore</b> <b>Machines</b>	<b>Start date or starting event:</b>			M0
<b>Activity Type</b> <b>RTD</b>	<b>10</b> <b>AMOLF</b>	<b>3</b> EPFL	<b>7</b> ETH	<b>1</b> FZK-INT	
<b>Participant id</b>					
<b>Person-months per participant:</b>	14	6	6	15	

**Objectives**

**O5** Fully comprehend the **dynamics** of the *biologically*-active, pore systems and use this knowledge to design *synthetic molecular nanopore mimics*.

**Description of work**

Protein-importing molecular motors perform the intriguing task of protein recognition, grabbing a folded protein, unfolding it, translocating it across a cellular membrane, after which it refolds again. This motor functions in membranes have not yet been investigated at the single molecule level. Our studies focus on the bacterial Sec system, which is considered a model system for the many other (also human) existing protein-import motors. Laser tweezer techniques are ideal tools to get further insight into the dynamics and working mechanisms of such nanopore machines. The gained knowledge will be the base for the construction of simple biomimetic models for nanopores performing crucial tasks as protein recognition, substrate grabbing and size adaptation.

**Deliverables**

**D5-1** M18 Single-Motor Measurements of movements and forces involved in protein translocation (report)

**D5-2** M36 Design and synthesis hexameric spin transition Fe<sup>II</sup> compound (report)

**Milestones and expected results**

**M5-1** M06 Establish efficient translocation into vesicles on a surface, using biochemical assay

**M5-2** M14 Establish procedure for firm attachment of vesicles to surface

**M5-3** M18 Ligand synthesis for hexameric Fe(II) compound

**M5-4** M30 Reduce various unwanted non-specific interactions, e.g. between bead surfaces.

**M5-5** M34 Design and structural characterisation of the [5] catenane

## Nanopore Machines

### Introduction

Embedded in cellular membranes one finds molecular motors that fulfil the intriguing task of grabbing a folded protein, unfolding it, and translocating it across the membrane. Without this activity cellular systems and organelles could not exist. Cellular organelles rely on import because they cannot synthesize the proteins they use inside. Aberrant protein translocation and folding have been linked to hereditary diseases like primary hyperoxaluria, which causes kidney stones at an early age and some forms of inherited high cholesterol, as well as illnesses like cystic fibrosis.

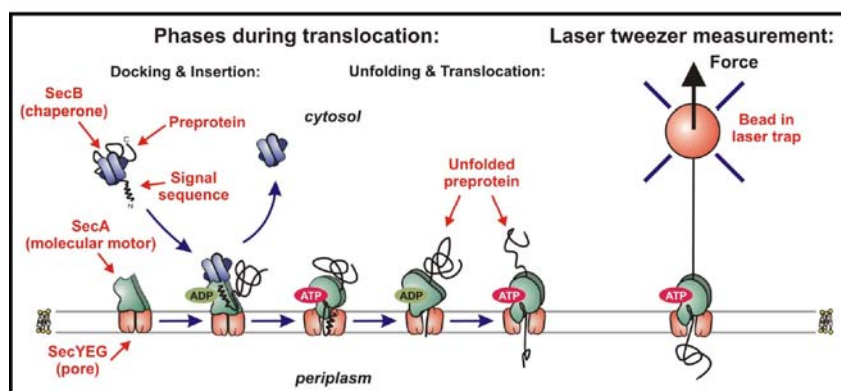


**Figure 17.** Schematic of protein translocation across a cellular membrane, and the measurements of an individual translocation event using optical tweezers.

Of the bacterial Sec translocase, a detailed knowledge of its components and their interactions has been obtained from biochemical and genetic studies (Fig 17 and 18). A picture emerges of an intriguing and highly dynamic process in which cycles of ATP binding and hydrolysis by the SecA motor drive the step-wise translocation of the preprotein through the SecYEG pore. However, the more detailed picture is puzzling and controversial. The main reason for this is that biochemical assays cannot address molecular movements and forces. Further progress in the understanding of protein translocation crucially depends on knowing how the molecules actually move. Here we aim to address these issues by molecular dynamics simulations of the translocation motor, as well as by direct measurements using optical tweezers.

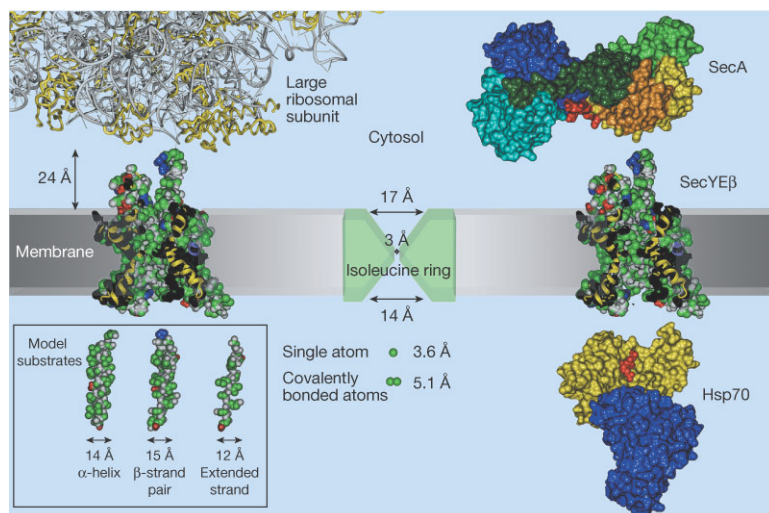


**Figure 18.** Atomic structure models of protein translocation machines (from: van den Berg et al, Nature, 427, 2004)

## Molecular dynamics simulations of a protein translocation motor (EPFL)

The ATPase protein SecA is the “motor” that drives the bacterial protein secretion system. By successive ATP binding cycles the SecA protein is able to transform chemical into mechanical energy and translocate proteins across the periplasmatic membrane. Starting from a recently determined crystal structure from *Bacillus Subtilis* [1] (PDB 1TF2), molecular dynamics simulations using the Amber force field performed in our laboratories show a large conformational change when ADP is replaced by ATP in the binding pocket. As we are only interested on the long time, large amplitude motion, conformational analysis is performed using as initial configuration a 1ns ATP bound structure. This procedure also ensures that the relative arbitrariness of the initial ATP bound structure will not influence the results.

Figure 19 shows the results of the protein domain motion [3] analysis comparing trajectory frames at 1 nanosecond (ns), with frames at 13ns and 20ns. The protein domain analysis agrees with the essential dynamics results from our trajectories and show that the major ATP-induced conformational change is associated with a concerted turn of several protein domains on the opposite side to the *nucleotide binding folds* (NBF). The results also show that (a) the SecA’s long 49 residues alpha helix that belongs to the alpha *helix scaffold domain* (HSD) is considerably strained during the process (Figure 20) and (b) the turning axes points in a direction that is almost parallel to the direction of the long alpha helix. This points to a motor mechanism in which the ATP-induced local conformational change, more specifically the angle change between the *nucleotide binding folds* I and II (NBF-I and NBF-II), causes a global conformation change in the protein with the long alpha helix acting as a transmission axis.

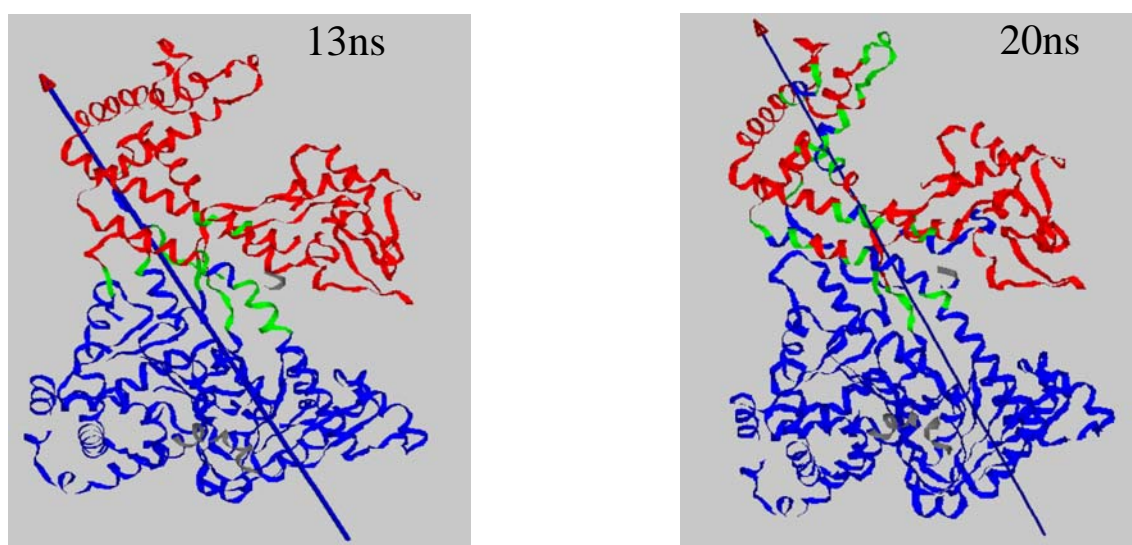


**Figure 19.** ATP-induced conformational changes as obtained by the Dyndom analysis when comparing 1ns vs. 13 and 20 ns structures.

### *Towards single-molecule measurements of protein translocation (AMOLF)*

**M5-1 “Establish efficient translocation into vesicles on a surface (M06)” and**

**M5-2 “Establish procedure for firm attachment of vesicles to surface (M14)”**

In order to measure translocation of single proteins, we must show that we can attach them to microspheres that serve as handles to manipulate them, as shown in figure 20. The same holds for the membrane vesicles, in which the translocons reside, at the other end of the construct. Here we report on our results for several routes that we have tested for these attachments. The report shows that all desired attachments have been achieved, but that an aspecific interaction between the preproteins and the vesicles needs to be reduced, for which we outline several possible solutions.

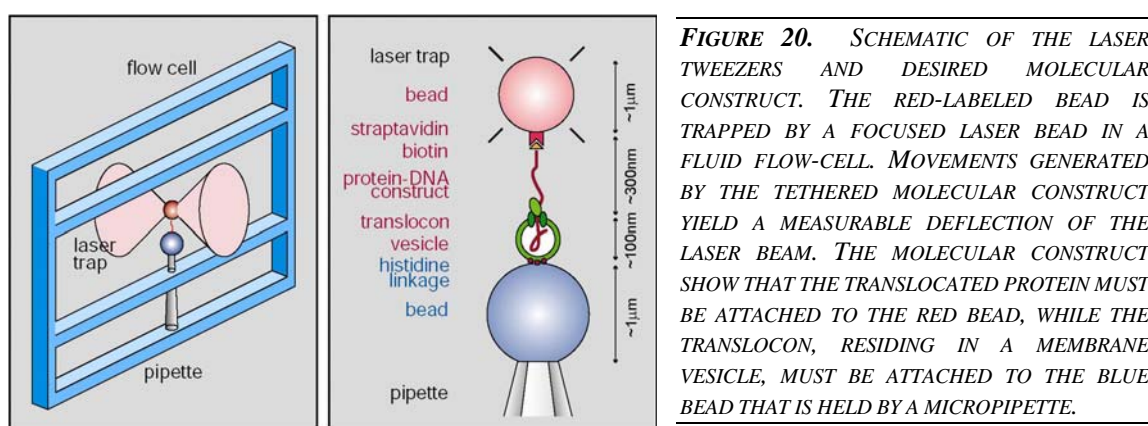


**FIGURE 20.** SCHEMATIC OF THE LASER TWEEZERS AND DESIRED MOLECULAR CONSTRUCT. THE RED-LABELED BEAD IS TRAPPED BY A FOCUSED LASER BEAD IN A FLUID FLOW-CELL. MOVEMENTS GENERATED BY THE TETHERED MOLECULAR CONSTRUCT YIELD A MEASURABLE DEFLECTION OF THE LASER BEAM. THE MOLECULAR CONSTRUCT SHOW THAT THE TRANSLOCATED PROTEIN MUST BE ATTACHED TO THE RED BEAD, WHILE THE TRANSLOCON, RESIDING IN A MEMBRANE VESICLE, MUST BE ATTACHED TO THE BLUE BEAD THAT IS HELD BY A MICROPIPETTE.

### **Protein attachments (AMOLF)**

The translocated protein that have been tested contained the following necessary ingredients:

- 1) attachment site on C-terminal end, for linkage to bead. In order to have a flexible construction, we have chosen for a biotin group for this function, which would allow both for a direct linkage to the bead, as well as an indirect linkage via a DNA tether (see Figure 21).
- 2) signal sequence on N-terminal end, for recognition by translocon.
- 3) increased length for significant measurement time. We tested a protein with an 8-fold repeated domain, as designed at the level of the DNA that encodes the protein (see figure 19). The repeated domain also will likely yield repeated features in the eventual translocation measurements.
- 4) Additional spacer or tether between bead and protein to prevent interference of pipette bead with laser beam. For this purpose we used a DNA tether of roughly 2 microns length. The best results were obtained with a DNA linker with DIG groups on one end, and a biotin group on the other. We then used a anti-DIG antibody coated bead as the trapped bead, while a streptavidin molecule served as a bridge between the DNA tether and the protein.

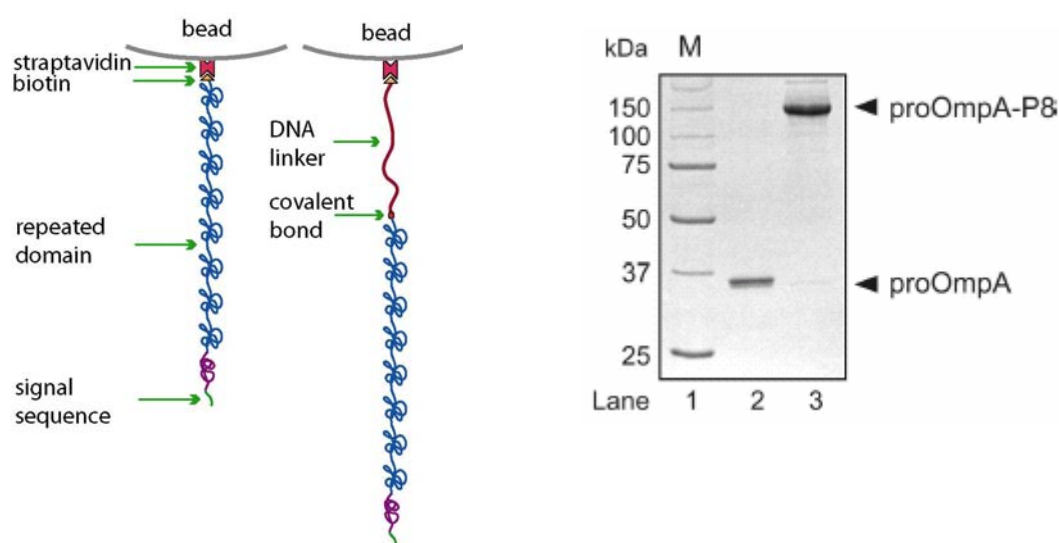


**FIGURE 21.** SCHEMATIC OF THE PROTEIN CONSTRUCTS, AS WELL AS A GEL SHOWING THE ORIGINAL MODEL PROTEIN PROOMP A AND THE PROOMP A-P8 OR P8 CONSTRUCT THAT HAS AN 8-FOLD REPEATED DOMAIN.

### Vesicle attachments (AMOLF)

The vesicles can be seen as ‘balloons’ made of actual cell membrane material. The cells from which they are made are genetically modified to overexpress the translocation channel, such that all vesicles, which have been sized to a diameter of about 100nm, contain 1 or more translocation channels. In order to attach these vesicles to the blue-labeled bead, we mainly tested 2 different routes. In the first, we tested vesicles with HIS-tagged labeled translocation channels. These HIS tags, which can be introduced at the level of the DNA in the cell that encodes the channels, can be bound to anti-HIS-antibodies. These antibodies were purchased and covalently bound to the beads using a standard chemical protocol. However, we found that this desired linkage was not able to form for unknown reasons. One possibility is that other, such as electrostatic, interactions between the vesicles and the beads were of a repelling nature. Given these results, we then aimed to exploit these possible electrostatic interactions: vesicles are predominantly negatively charged, and we thus tested positively charged amine coated beads. This combination yielded good results, as illustrated by a fluorescence assay testing for vesicles on beads (Fig. 22).



**Figure 22.** Assay showing that the vesicles attach to amine beads. These vesicles were biotinylated, and made visible with fluorescently labeled streptavidin. Coating of the beads with the blocking agent BSA yielded much less fluorescence intensity.



### Measuring attachments using optical tweezers (AMOLF)

In order to obtain the complete construct, all components must be brought together. Whether indeed the molecular construct can bridge the two beads, can be tested in the laser tweezers apparatus, of which a schematic is given in figure 23. Note that many of the attachments do not require other reagents, which means that we have a large freedom in putting all the elements together. In these tests, the beads that are dressed with molecules are brought together with the tweezers so that the bridge can form. As the beads are separated again, a measured force on the trapped bead will indicate a linkage to it. By separating the beads further the applied force will increase. At a certain force the construct will break, giving an indication of the attachment strength. We will now summarize the results of several routes of construction that we have tested.

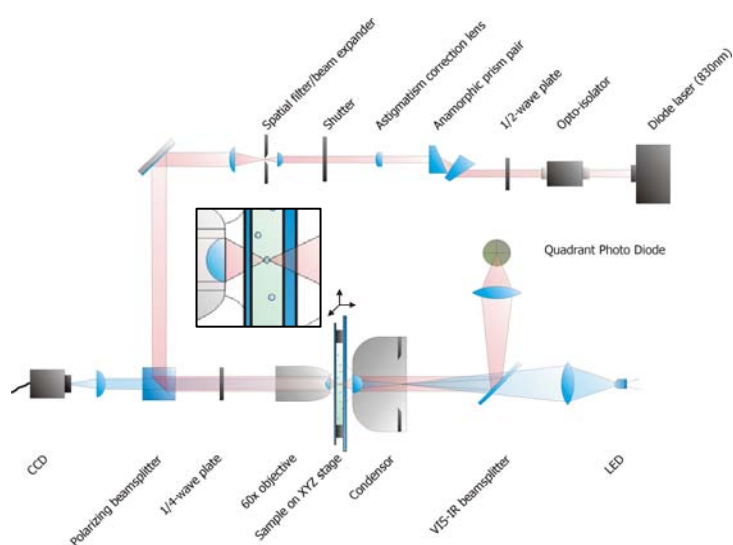
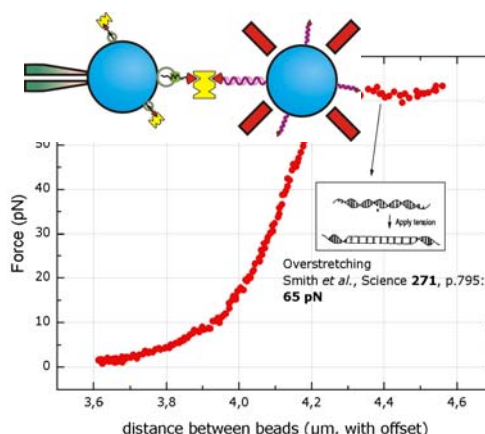


Figure 23: schematic of the laser tweezers set-up. The laser output (red) is first shaped to a gaussian beam, and then focused by a 60x water immersion objective. The focus inside the liquid-filled flow-cell traps the microspheres that have a different refractive index. A condenser collects the light and projects it on a quadrant photo detector, which detects deflections of the laser beam.

Figure 24: Laser-tweezers measurement evidencing that the molecular construct bridges the two beads. This bridge is able to support the force required for overstretching the DNA. Inset: desired construct, showing the preprotein inserted into the vesicle, and attached to the DNA linker via streptavidin (yellow). The DNA is attached to the bead via a DIG-antiDIG interaction.



First we tested the two DNA linkages alone, using DIG-antibody coated beads and streptavidin coated beads. We found that with multiple DIG groups incorporated in one DNA-end, using standard PCR and ligation, very strong and specific attachments could be made that reached beyond the overstretching transition of about 65pN. Next, we tested the Attachment strength of the vesicles to the amine beads by using biotinylated vesicles, to which we could connect with the DNA tether. Again, strong tethers were able to form beyond the overstretching transition, showing that the vesicles attached strongly as well (M5-2).

In order to better control the protein insertion process, we developed a protocol that does not rely on uncertain insertion in the tweezers apparatus. In this protocol, proteins were partially translocated in bulk, and prematurely stopped by the addition of ATP-Gamma-S, which does

not hydrolyze. In this fashion we could produce vesicles that should have the biotin group of the partially translocated protein exposed to the outside.

Using the sucrose cushion method, we were able to purify –in bulk- excess streptavidin away from the rest of the components (see inset Fig. 24). The effect of this purification step was measured in the laser tweezers, by a marked decrease in aspecific tethers which would form even in the absence of vesicles on the amine beads. Later, we obtained even better purification results by first attaching the vesicles to the beads, followed by spinning down the beads. With the aim to reduce the unwanted aspecific interaction of the streptavidin to the amine beads, we tested the protocol of first adding the streptavidin to the DNA coated anti-DIG beads, followed by washing. We found that in this manner, unwanted aspecific attachments were not able to form.

Furthermore, from several construction routes we could conclude that the P8 protein is able to make aspecific interactions to the vesicles. For instance, without adding the ATP that drives the insertion, bridges between the beads were still able to form. A candidate for this interaction is the hydrophobic beta-barrel domain in the protein, which is present as one copy just after the signal sequence. Because molecular bridges with this interaction will mask the translocation activity, we have identified several ways to deal with this issue. Among those is the tuning of the excess P8, to optimise the specific interactions. Also, we aim to make a new protein construct that lacks the beta barrel domain.

### Translocation into vesicles on a surface (AMOLF)

In order to investigate whether the vesicles attached to the surface, were still active in translocation (**M5-1**), two bulk measurements were performed. The first consists of a protection assay, where after the translocation reaction protein outside the vesicles is digested with proteinase. After lysis of the vesicles, one can quantify the translocated protein on gel (Fig. 25, left panel). The second involves the quantification of ATP consumption, during the translocation process, which also is an accurate indicator of translocation activity.

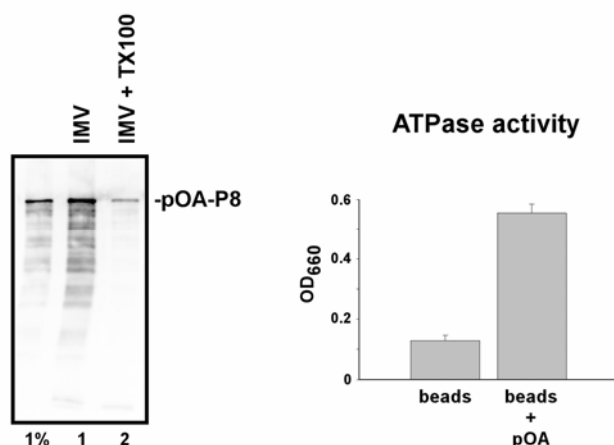


*Figure 25: Bulk experiments, protection assay and ATPase activity assay, showing translocation is efficient on the surface of amine beads.*



## Artificial synthetic nanopore mimics (FZK-INT)

### M5-3 “Ligand synthesis for a hexameric Fe(II) compound (M18)”

The rationale of the *de novo* design of nanopore-actuators inspired by the biological systems relies on the 10% lengths change of the Fe-N distance in spin transition Fe<sup>II</sup>-oligopyridyl be the design principle for “breathing” nanopores which are able to change their internal diameter triggered by external parameters. Since the Fe<sup>II</sup>(low spin)-N bond length averages 0.2 Å shorter than the Fe<sup>II</sup>(high spin)-N bond distance with  $d(\text{Fe}(\text{high spin})-\text{N}) = 2.0 \text{ Å}$ , the triggered switching between the two spin states can be used to change effectively the internal diameter of the nanopore mimics by environmental parameters (light, temperature, pressure).

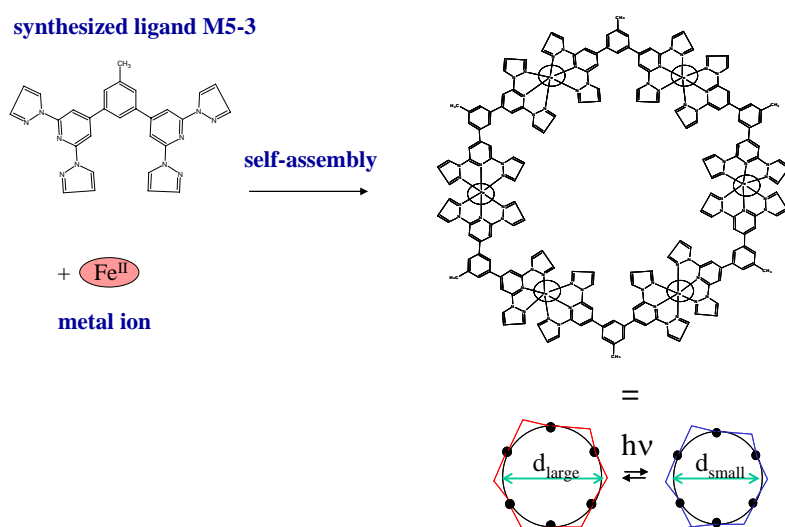


**Figure 26.** Synthesized ligand system (left, **M5-3**) and planned next steps to realize artificial nanopore mimics (**FZK-INT**)

Towards this goal, first an organic ligand system has to be synthesized. This ligand system has to fulfill two different tasks: (i) it has to steer self-assembly process via the coordination of Fe(II) ion in solution towards a belt-like, hexameric compound and (ii) it has to set the coordination parameters around the Fe(II) ion into a region, where the switching event spin transition is possible. The BIOMACH-partner **FZK-INT** has designed and synthesized a ligand system (see Figure 26), which can fulfill both conditions to reach such a nanopore-like functionality. In the next step, the self-assembly process has to be carried out and the functionality of the system will be studied.

### Conclusion

In conclusion, translocation activity on surfaces, specific and strong linkages of the protein and vesicles to beads has been achieved, fulfilling the milestones and objectives (**M5-1**, **M5-2**, **M5-3** & **D5-1**) for this period. After realizing further improvements to the aspecific P8-vesicle interactions, we can begin looking for movements generated by the protein translocation machinery and for the self-assembly of the artificial systems.

<b>Workpackage number WP6</b>	<b>Biomolecular motors on nanostructures</b>	<b>Start date or starting event:</b>			M 0
<b>Activity Type</b>	<b>RTD</b>	<b>8</b>	4	3	10
<b>Participant id</b>	<b>ICG-GC</b>	TU/d-MB	EPFL		ETH
<b>Person-months per participant:</b>	15	16	6		3

**Objectives**

**O6** Construct kinesin-motor based **biological-inorganic hybrid devices** for controlled nano-transport processes.

**Description of work**

The Delft group has extensive experience in nanofabrication and is now moving into single-molecule studies of motor enzymes. For a start, we will make linear extended nanostructures that will act as an optical grid. This connects to recent work from the Paris group who has developed a new technique to characterize single kinesin motors without any external force and at unprecedented bandwidth allowing in principle microsecond time resolution. Currently this involves the use of optical-interference patterns, but this will be replaced by a solid-state nanofabricated structure, which will allow a wide range of spacings in the pattern down to the few 10 nm range, and an improved stability. Kinesin motility will then be measured at the single molecule limit. The technique combines nm spatial and  $\mu$ s time resolution. New physics relating to the mechanism of kinesin motion is expected.

We will furthermore explore other possibilities where nanostructures can be useful to study biomolecular motors, or vice versa, where biomotors can be engineered in a useful way on nanostructures.

**Deliverables**

**D6-1** M12 Microtubules assemblies on nanostructures (report)

**D6-2** M36 Motility of single kinesin motors on these assemblies (report)

**Milestones and expected result**

**M6-1** M08 Nanofabrication of a variety of nanostructures on coverslips

**M6-2** M12 Assembly of microtubules on these structures

**M6-3** M24 Biophysical studies of the kinesin-microtubule system with the use of these nanostructures

**M6-4** M36 Exploration of additional hybrid systems with inorganic nanostructures and biomolecular motors

## Biomolecular Motors on Nanostructures

### *Introduction*

The biological cell utilizes motor proteins for the active transport of material. For example, the kinesin-microtubule complex is essential in intracellular transport, mitosis and many other biological processes: the kinesin motor proteins can bind to a cargo and walk along microtubules, which are long and stiff tubular proteins. One single kinesin moves processively along the microtubules by discrete steps of 8 nanometers, which corresponds to the microtubule periodicity, and it develops a force up to ~7 piconewtons.

The *scientific* focuses of these studies are, on one hand, the achievement of detailed kinematical description of the kinesin movement. This is essential to understand the mechanism of energy conversion used by the molecular motors: the experimental results will be compared with the microscopic models, which have been solved by analytical and numerical methods. On the other hand, we want to explore the use of biomolecular motors as transporters in nanotechnology, profiting their natural ability in organizing networks of lipids/microtubules and pulling vesicles and nano-tubes out of liposomes.

The *technical* aim of this project is to fabricate a substrate that integrates the nanostructures and a bio-compatible layer, in order to attach the microtubules to the pattern, and to set up a detection technique allowing us to follow the kinesin motion with high spatial and temporal resolution.

### *Objectives*

The objective for the first year was to fabricate a wide variety of solid-state nanostructures on the coverslips and to set up a fast tracking technique (M6-1), in order to supply new tools to manipulate the kinesins and follow their motion with an increased space-time, and to be able to assemble the microtubules on these structures (M6-2 and D6-1).

In the following paragraphs we will explain how the structures have been realized and characterized and we will show way to combine them with the motor proteins.

### *Nanofabrication and detection technique (M6-1)*

The micro-fabricated structures, with different size and shape, have been supplied by **TU/d-MB** and they have been characterized both by Scanning Electron Microscopy (**TU/d-MB**; Figure 27) and by Optical Microscopy (ICG-GC, Figure c).

Simultaneously, a new interference approach has been developed in the **ICG-GC** group: the Traveling Wave Tracking technique (*TWT*). In this technique, a particle is moving through the *traveling* interference pattern; the measurements of the intensity and phase of the scattered light allow to precisely track the particle and to measure simultaneously the position  $x$  (parallel to the surface) and the distance  $z$  between the particle and the surface. This method seems to be really promising because it allows great spatial and temporal resolution and an improved stability: the particle can be localized with sub-nanometer precision at the microsecond range (Figure 1).

A second and improved setup for *TWT* is being built at **TU-Delft** that will complement the one at the Institut Curie (**ICG-GC**). The initial design is based on the setup at the **ICG-GC**. It will have several improvements with the idea of obtaining a better stability, resolution and signal to noise ratio. A future goal would be to expand the capabilities of this system to track not

only displacements in 2 directions but in 3 directions with a time resolution above 30 kHz. Vibration isolation is very important, for that we are setting up a new active optical table and, in order to reduce other sources of noise, most of the setup will be in a box under controlled atmosphere and the illuminating laser be coupled to the experiment by the use of optical fibers.

Other changes will include the conjugation of the motors to gold nanoparticles, in order to take advantage of their large scattering intensity at small dimensions (M6-4). With these improvements we hope to obtain sub-nanometer resolution with a large bandwidth.

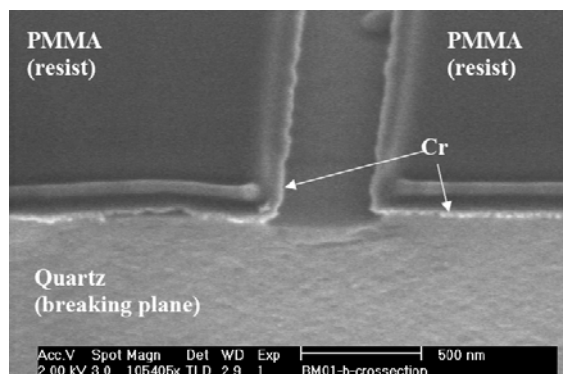


**Figure 27.** SEM image crosssection of 300 nm wide trench. Image was taken in an intermediate stage of the processing. On top of the quartz there is first ~35 nm of Cr, and then ~200 nm of PMMA (e-beam resist). The SEM image perspective should be compared to the schematic drawing. The rounded trench bottom and the under etch under the Cr layer can be observed.

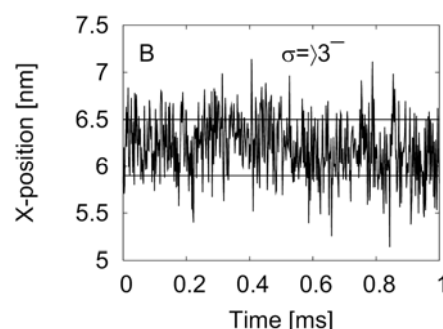
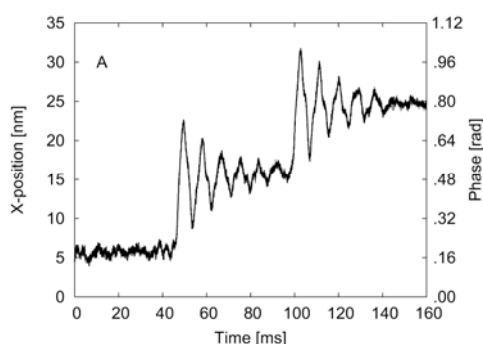


**Figure 18.** A) A single colloid (diameter 200 nm) is fixed on the coverglass, while the sample holder is moved in 10 nm steps by means of a calibrated piezoelectric stage. B) the residual shot noise limits the resolution to 3 Angstroms RMS.

#### *Assemble the microtubules on the structures (M6-2 and D6-1).*

At **TU/d-MB**, and in collaboration with the **ICG-GC**, several structures have been designed and tested. The new structures are designed with the idea of letting the object of study move freely in 3 dimensions and not be constrained by a surface in such a way that the beads used for tracking can move around the object under study. With that purpose in mind, the different structures involve the definition of some kind of trench or hole, with dimensions varying from 300 nm to 1.5  $\mu\text{m}$  on the side, onto which the various molecules under study can be

suspended. The samples are created using electron beam pattern generator where, with high resolution, several test structures are defined and are such that there are many shape combinations on one chip. 29 (a) and (b) display side views of typical configurations of the samples tested. Two different approaches were used one based on all glass and the other one, metal on glass. 29 (c) displays a test under *TWT* illumination for a metal on glass sample where scattering from the side of the trenches can be observed in one direction but not in the perpendicular direction.

The possibility to attach microtubules on soft nanopillars (PDMS) has also been explored at ICG-GC, as shown in 30.

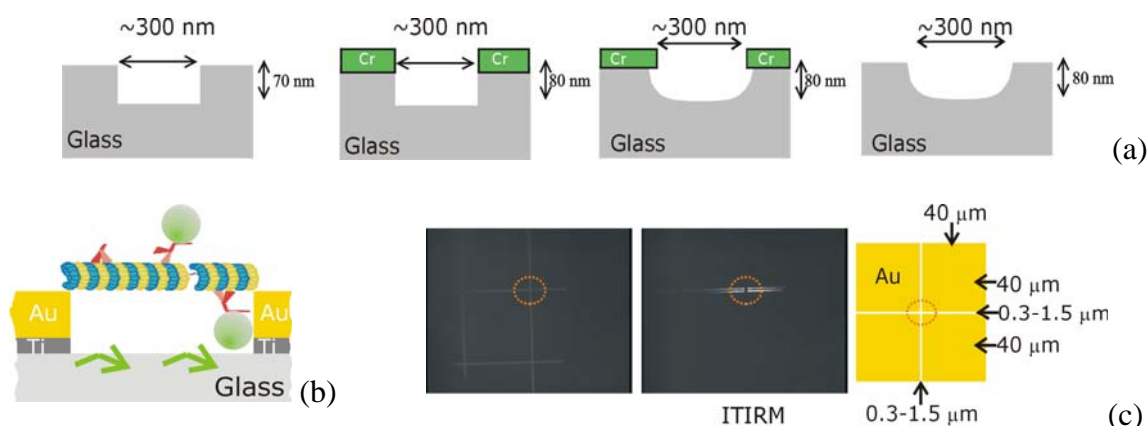


**Figure 29 :** *a)* many different nanostructures have been tested with different features. *b)* a schematic view of the experiment: the microtubules are attached to the structures and the motors freely move along the tubes. *c)* total internal reflection microscopy on the nanofabricated structures.

The use of those biomolecular motors as transporters in nanotechnology has been explored in the **TU-d-MB** group. Nanofabrication techniques and specific chemical absorption have been used to create tracks for microtubule shuttles. Gold-covered trenches in silicon-oxide ( $\text{SiO}_2$ ) chips (Figure ) are created by using a combination of e-beam lithography, reactive-ion etching and e-beam evaporation. The kinesin molecules only absorb on the gold covered trench bottoms. Microtubules can be visualized moving only over the gold areas using fluorescence microscopy (Figure ).

The experiments also demonstrated the localized electrical control of the docking of microtubules onto engineered kinesin-coated structures. After applying a voltage to a gold electrode, we observe an enhanced transport of microtubules from solution towards the surface, and a subsequent increased amount of moving microtubule shuttles (Figure 29). Switching off the voltage leads to a partial detachment of microtubules from the surface. The area coverage of microtubules, during both the docking and undocking events, follows exponential time dependence (Figure 30). We have developed a simple kinetic model, incorporating the equilibrium between free and surface bound microtubules, to explain these data.

**Figure 30 a.** microtubules attached on top of PDMS nanopillars

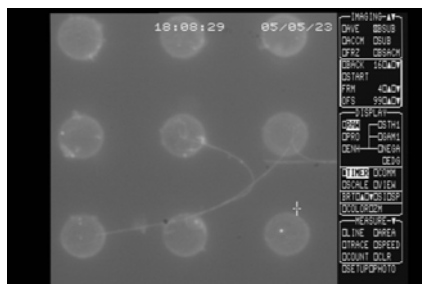


**Figure 30 b.** Scanning electron microscope picture of a nanostructure

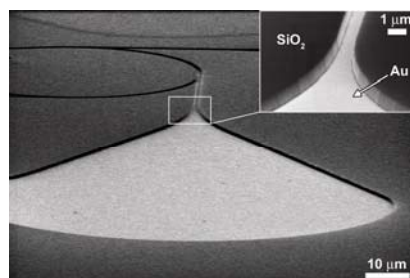


**Figure 30 c.** Fluorescence image showing microtubules moving over the gold, but not over the SiO<sub>2</sub>

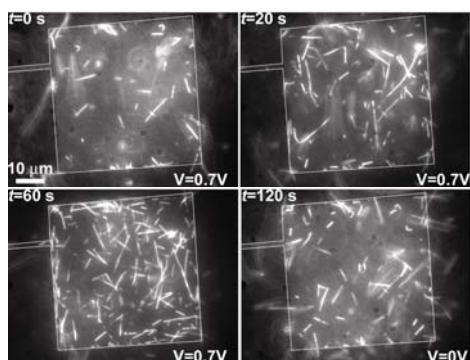
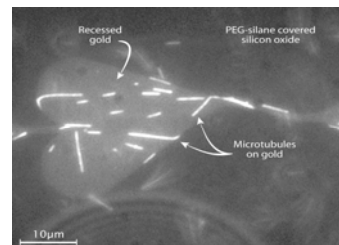


**Figure 30d.** Time-lapse of fluorescence images showing microtubules docking onto a gold electrode upon application of a voltage.

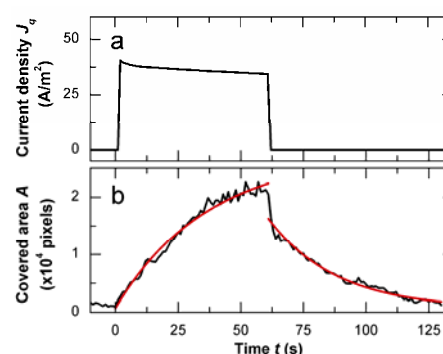


**Figure 30e.** Timetraces of current density (a) and microtubule density (b) corresponding to the event shown in figure 26.

## Conclusion

Many different nanofabricated structures were made in **TU/d-MB** and their optical features have been measured by total internal reflection microscopy (**M6-1**). As the electromagnetic field near the structures is poorly known, we decide to develop a more flexible optical technique, called *Travelling Wave Tracking* (**ICG-GC**). In such a way the nanostructures are not further used as an optical tool, but they will serve us as a three dimensional holder for the microtubules.

The microtubules have been injected in the structures (**TU/d-MB**) and the activity has successfully been checked (**D6-1** and **M6-2**).

In conclusion, the objectives for the first year have been achieved and we can begin measuring single molecular motors moving on the suspended microtubules.

## BIOMACH at the MTRW M18 – Conclusion and Outlook

During the first 18-months period, the BIOMACH consortium successfully implanted the scientific and management collaboration between four different scientific communities, which, although altogether dealing with “Molecular Motors”, acted so far more as separated subgroups. The first and most important task has been to initiate a true cross-disciplinary discussion, which was achieved by a multitude of scientific meeting at different levels of participation. Furthermore, the first two- or three-centre collaboration projects were started along the milestones of the project given in the working plan of the BIOMACH project.

Altogether, **twelve** milestones and **five** deliverables could be achieved in time (see Figure 31). It can be concluded that the BIOMACH project is following the foreseen working path and no severe deviation has been detected, so far. Several **collaboration clusters** have been formed: MPI-FKF / ULP / FZK-INT around WP 1, WP 2 and WP 3; CIAM / ETH and MPI-FKF / FZK-INT within WP 4; AMOLF / EPFL and AMOLF / FZK-INT within WP 5 and ICG-GC and Tu/d-MB within WP 6. It is planned to continue and to deepen this process by the interconnection of the different Wp's. Especially, the interaction between the biological and the artificial systems and between experimental and theoretical approached will be underlying special attention.

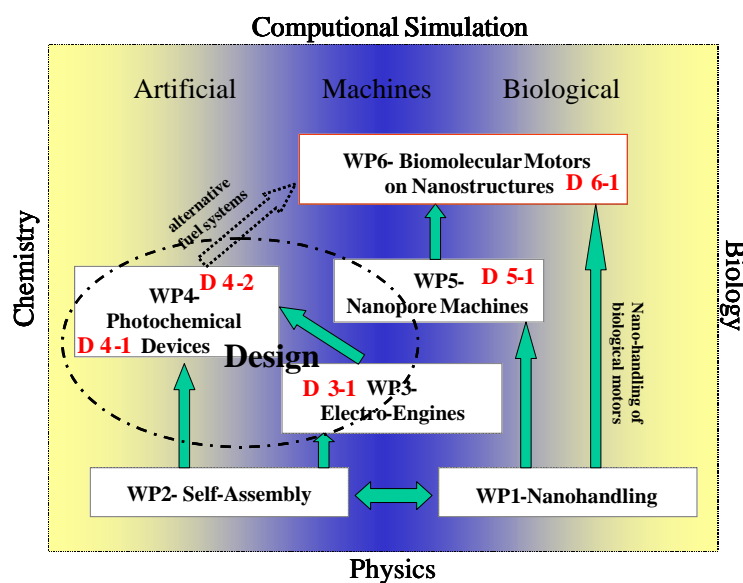


**Figure 31.** The working plan of the BIOMACH-Project with supplied deliverables at M18 (Midterm Review Meeting)

It can be stated that the BIOMACH project has set up the necessary management conditions and has initiated an intense, cross-disciplinary scientific discussion and collaboration process. The work on the next pivotal (because of the strategic position of WP 1 and 2) deliverables D1-1 and D2-1 has been started. Based on the so far obtained results, cutting edge research as leading European contribution to the perspective field of “Molecular Motors” can be expected from the BIOMACH consortium during the second half of the funding period.



## BIOMACH Plan for using and disseminating the knowledge

### Section 1 - Exploitable knowledge and its Use

So far, no commercially exploitable knowledge e.g. (patents, design rights, database rights, plant varieties, etc.) was generated.

### Section 2 – Dissemination of knowledge

As cornerstones of the dissemination strategy, the BIOMACH consortium is heavily involved into the realisation of the two management deliverables due to the Mid-term Review Meeting (M18).

<b>DMa 1</b>	<b>BIOMACH conference on nanomotors and bioengines</b>	<b>Man.</b>	<b>BIOM.</b>	<b>3</b>	<b>O</b>	<b>PU</b>	<b>M18</b>
<b>DMa 2</b>	<b>Creation of BIOMACH-website</b>	<b>Man.</b>	<b>BIOM.</b>	<b>12</b>	<b>O</b>	<b>PU</b>	<b>M9</b>

The organisation of the BIOMACH conference (**Deliverable DMa-1**) reviewing the world-wide progress on the field of molecular motors has started. The conference will take place 18<sup>th</sup>- 23<sup>rd</sup> September 2005 at the Conference Centre of the ETH Zürich in Ascona/Switzerland. A speakers list was established by the BIOMACH Project Steering Committee (see Annex III) and the invitation were send out as early as August 2004 to guarantee high-quality participants.

The construction of the BIOMACH website (**Deliverable DMa-2**) as reference point in the field of molecular motors and engines has well progressed and the access to the full content of [www.biomach.org](http://www.biomach.org) was achieved preliminarily and is online since **M09**.

### Section 3 - Publishable results

Scientifically, so far, **ten publications** have been published and two more publications are in preparation, so far. Preliminarily, results were presented on several conferences (19) mostly in Europe and also in overseas.

Additionally to the planned deliverables, **three press releases** are supporting our dissemination strategy. A first one was prepared to present the BIOMACH Project at après conference on the EuroNano21 conference from 13<sup>th</sup>-17<sup>th</sup> December 2003 in Trieste/Italy. A second press release was prepared together with the EC in order to present the BIOMACH Project on the EC web sites and third one was published in the “**Parliaments Magazine-European Politics and Policy**” in June 2005.